

Background Document

FEMA P-58/BD-3.7.21

Simplified Analysis Response Models for SCBF and BRBF Compliant with FEMA P-58 Simplified Procedures

Prepared by

Daniel Saldana and Vesna Terzic
California State University, Long Beach
Department of Civil Engineering and Construction Engineering Management
Long Beach, California 90815

Submitted to

APPLIED TECHNOLOGY COUNCIL
201 Redwood Shores Parkway, Suite 240
Redwood City, California 94065
www.ATCouncil.org

Prepared for

FEDERAL EMERGENCY MANAGEMENT AGENCY
U.S. Department of Homeland Security
500 C Street, SW
Washington, D.C. 20472

March 2018



FEMA



Background Documentation

FEMA P-58 Background Documents are a series of reports documenting the technical background and source information for key aspects of the FEMA P-58 methodology and its implementation. This report was developed over the course of the 5-year ATC-58-2 Project funded under FEMA Contract HSFE60-12-C-0243.

Background Documents were developed by consultants, serving at various levels within the project hierarchy, reporting the results of: (1) decisions on technical development protocols; (2) focused studies on the development of key aspects of the methodology; (3) documentation of recommended procedures; and (4) collection of available data for the development of structural and nonstructural fragilities. They were initially intended to serve as a record of the technical state-of-knowledge at the time they were produced, and as resources for the development of the eventual project reports. As such, they represent a snapshot in time, and may, or may not, match the technical content, recommended procedures, or data incorporated into the final methodology and its implementation.

This Background Document is intended for the purpose of providing supplemental knowledge to users of the FEMA P-58 methodology. Information contained herein has not been independently verified for accuracy as a stand-alone document, and may have been superseded in its final implementation within the methodology. Specifically in the case of certain nonstructural component fragilities, the NISTIR fragility classification numbering scheme was modified over the course of the project, and the fragility classification number assigned in this document might be different from numbers assigned in the final fragility database. Users of information in this document assume all liability arising from such use.

Notice

Any opinions, findings, conclusions, or recommendations expressed in this publication do not necessarily reflect the views of the Applied Technology Council (ATC), the Department of Homeland Security (DHS), or the Federal Emergency Management Agency (FEMA). Additionally, neither ATC, DHS, FEMA, nor any of their employees, makes any warranty, expressed or implied, nor assumes any legal liability or responsibility for the accuracy, completeness, or usefulness of any information, product, or process included in this publication. Users of information from this publication assume all liability arising from such use.

Cover photograph – Primary resource documents for the FEMA P-58 *Seismic Performance Assessment of Buildings, Methodology and Implementation* series of products: FEMA P-58-1, *Volume 1 – Methodology, Second Edition*, and FEMA P-58-2, *Volume 2 – Implementation Guide, Second Edition*.

Simplified Analysis Response Models for SCBF and BRBF Compliant with FEMA P-58 Simplified Procedures

Daniel Saldana and Vesna Terzic

Introduction

This report provides simplified analysis response models for buildings that utilize either special concentrically braced frame (SCBF) or buckling restrained braced frame (BRBF) as a lateral load-resisting system. The presented models are developed in accordance with the simplified response analysis procedures established by Huang and Whittaker (2012) to aid performance-based seismic assessments of FEMA P-58 (FEMA, 2012). The models can be used to estimate median nonlinear inter-story drift, peak (total) floor velocity, and peak floor acceleration given spectral demands and rudimentary knowledge of the structural system.

Numerical models and ground motions

Table 1 lists buildings used in this study considering two lateral load-resisting systems, SCBF and BRBF, and the following building heights: 3-, 6-, 12-, and 16-stories for each system. Two building designs are considered for each story height, a minimum-code design and above-code stiffer building design. The fundamental periods of the considered buildings range from 0.58 seconds (3-story SCBF) to 5.0 seconds (16-story BRBF). Building designs and their nonlinear analytical models are adopted from Chen and Mahin (2012). Opensees computation software is used for structural analysis of the considered buildings. Response history analyses were performed using two bins of ground motions, near-fault and far-field, which were assembled for the FEMA P-58 ground motion studies (Huang et al., 2011). Each set of ground motions contained 25 pairs of seed ground motions. To achieve wide range of shaking intensities, the selected set of ground motions was amplitude-scaled by 0.1, 0.5, 1.0, and 2.0.

Acceleration, velocity, displacement and drift notation within simplified analysis procedure of FEMA P-58

Figure 1 defines the story level, floor level, and story height used in the simplified analysis procedure. Notation used for peak floor acceleration, floor velocity, story drift, and roof displacement are listed below:

a_i^{in} Total floor acceleration at Floor i calculated by response – history analysis.

a_i^{si} Total floor acceleration at Floor i calculated by the simplified procedure before correction.

a_i^{si*} Total floor acceleration at Floor i estimated by the simplified procedure after correction.

v_i^{in} Total floor velocity at Floor i calculated by response – history analysis.

v_i^{si} Total floor velocity at Floor i estimated by the simplified procedure before correction.

v_i^{si*} Total floor velocity at Floor i estimated by the simplified procedure after correction.

Δ_i^{in} Drift in Story i (relative displacement of Floor i and Floor $i + 1$) estimated by response – history analysis.

Δ_i^{si} Drift in Story i (relative displacement of Floor i and Floor $i + 1$) estimated by the simplified procedure before correction.

Δ_i^{si*} Drift in Story i (relative displacement of Floor i and Floor $i + 1$) estimated by the simplified procedure after correction.

δ_r^{in} Roof displacement (with respect to the base of the building) calculated by response – history analysis.

δ_r^{si} Roof displacement (with respect to the base of the building) calculated by simplified – procedure.

Correction factors for estimating peak story drift compliant with the simplified analysis procedure of FEMA P-58

Within the simplified analysis procedure of FEMA P-58, the story-drifts are calculated by correcting the story drifts of story i , Δ_i^{si} , with a correction factors $H_{\Delta i}$ following Equation 1.

$$\Delta_i^{si*} = H_{\Delta i} * \Delta_i^{si} \quad i = 1 \text{ to } N \quad (1)$$

In this study, the correction factors are derived for two structural systems, SCBF and BRBF, utilizing the regression model recommended by Huang and Whittaker (2012):

$$\ln H_{\Delta i} = a_0 + a_1 T_1 + a_2 S + a_3 \frac{h_i}{H} + a_4 \left(\frac{h_i}{H} \right)^2 + a_5 \left(\frac{h_i}{H} \right)^3 \quad S \geq 1, i = 1 \text{ to } N \quad (2)$$

where i is the story number; $H_{\Delta i}$ is the story-drift corrections factor for Δ_i^{si} ; T_1 is the fundamental period of the building; S is the strength ratio of the building (refer to Equation 4); and h_i/H is the ratio of the height of floor i over the total height of the building.

To develop correction factors $H_{\Delta i}$ for Δ_i^{si} , residual values, $\ln(\Delta_i^{si}/\Delta_i^{in})$, were generated for all structural models, stories, ground motions and considered seismic intensities. Two separate regression analyses are performed for each framing system considering different building heights, one for 3- and 6-story buildings and another for 12- and 16-story buildings due to significantly larger number of residual values ($\ln(\Delta_i^{si}/\Delta_i^{in})$) for taller than for shorter buildings. For 3-, and 6-story buildings, the value of coefficient a_5 was set to zero. For 12- and 16-story buildings the cubic term for h_i/H is used to capture the higher mode effects.

Additionally the following two parameters, approximate story ductility (μ) and strength ratio (S) are used in the regression analysis to filter out the data that may be out of the possible range of a

structural response prior to the failure. For each structural model and ground motion, μ and S are calculated as follows:

$$\mu = \frac{\max(\Delta_i^{in})}{\Delta_y} \quad \text{where } \Delta_y = \frac{\delta_y}{H} \quad (3)$$

$$S = \frac{S_a(T_1, \xi_1)W}{V_{y1}} \quad (4)$$

and only values associated with S smaller than 10 and/or μ smaller than 6 for BRBF and/or μ smaller than 8 for SCBF were included in the analysis. The designations in Equations 3 and 4 are as follows: $\max(\Delta_i^{in})$ is the maximum story drift across the building estimated by response-history analysis; Δ_y is an approximate yield story drift calculated as the ratio of yield roof displacement (δ_y) over the total height of the building (δ_y is estimated by pushover analysis); $S_a(T_1, \xi_1)$ is the spectral acceleration at the fundamental period and damping ratio of the building for the ground motion used in analysis; W is the effective seismic weight of the building; and V_{y1} is the yield strength of the building estimated by pushover analysis considering the first mode distribution of seismic forces.

To calculate story drifts, Δ_i^{si} , a pseudo lateral load, V , was first computed for each of the considered ground motions and its equivalent lateral forces, F_x , were distributed along the building height. The force V is computed as follows:

$$V = C_1 C_2 S_a(T_1) W_1 \quad (5)$$

where $S_a(T_1)$ is the 5% damped spectral acceleration at the fundamental period of the building; W_1 is the first modal weight of the building which cannot be less than 80% of the total weight, W ; C_1 is an adjustment factor for inelastic displacements; C_2 is an adjustment factor for cyclic degradation. Coefficients C_1 and C_2 are calculated per *FEMA P-58*. For those ground motions for which a building remained elastic, the coefficients C_1 and C_2 were set to 1.0.

The equivalent lateral loads distributed over the building height with the lateral load at floor level x , F_x , were calculated as follows:

$$F_x = C_{vx} V \quad (6)$$

using the vertical distribution factor, C_{vx} :

$$C_{vx} = \frac{w_x h_x^k}{\sum_{i=2}^{N+1} w_i h_i^k} \quad (7)$$

where w_i (w_x) is the lumped weight at Floor i (x); h_i (h_x) is the height above the base of the building to the Floor i (x), as shown in Figure 1; and k is equal to 1 for structures with fundamental periods of 0.5 seconds or less and k is equal to 2 for structures with fundamental periods greater than 2.5 seconds (linear interpolation was used for intermediate periods).

For an elastic model of a building and a given ground motion characterized with its equivalent lateral load distribution, floor displacements and story drifts were next computed. These story drifts, Δ_i^{si} , are finally compared to the peak story drifts calculated by response history analysis utilizing a nonlinear building model subjected to the same ground motion, Δ_i^{in} . The ratio $\Delta_i^{si}/\Delta_i^{in}$ was generated for each of the considered buildings at all stories and all ground motions and utilized within appropriate regression model to derive the correction factors for estimating peak story drifts pertinent to simplified FEMA P-58 procedure. Table 2 presents regression coefficients a_0 through a_5 for 3-, and 6-story buildings and Table 3 presents regression coefficients for 12-, and 16-story buildings.

Figures 2 through 5 present results for $\Delta_i^{si}/\Delta_i^{in}$ for the 3-, 6-, 12-, and 16-story buildings, respectively. In the figures, the 84th, 50th (median), and 16th percentiles of the displacement ratios are presented as a function of story number. The presented results demonstrate significant differences between the maximum story drifts estimated by response-history analysis and those estimated by the simplified procedure before correction.

To demonstrate the effectiveness of the regression model utilized in this study the corrected story drifts, Δ_i^{si*} , were computed for all models and all ground motions with S smaller than 10 and/or μ smaller than 6 for BRBF and/or μ smaller than 8 for SCBF and the displacement ratios $\Delta_i^{si*}/\Delta_i^{in}$ are presented in Figures 9 through 12. Most of the median values of $\Delta_i^{si}/\Delta_i^{in}$ are significantly improved by correcting the displacement by utilizing the correction factor $H_{\Delta i}$. The only exception is the case where most of the building damage concentrates at one floor level, e.i., extensive buckling of braces is observed primarily at one story of a SCBF.

Correction factors for estimating peak floor velocity compliant with the simplified analysis procedure of FEMA P-58

Within the simplified analysis procedure of FEMA P-58, the floor velocities are calculated by correcting the total floor velocity at Floor i , v_i^{si} , with a correction factor H_{vi} following Equation 8.

$$v_i^{si*} = H_{vi} * v_i^{si} \quad i = 2 \text{ to } N + 1 \quad (8)$$

To develop correction factors H_{vi} for v_i^{si} , residual values, $\ln(v_i^{si}/v_i^{in})$, were generated for all models, stories, ground motions and considered seismic intensities. Only the values associated with S smaller than 10 and/or μ smaller than 6 for BRBF and/or μ smaller than 8 for SCBF were included in the regression analysis. The following regression model was used to develop corrections factors for v_i^{si} :

$$\ln H_{vi} = a_0 + a_1 T_1 + a_2 S + a_3 \frac{h_i}{H} + a_4 \left(\frac{h_i}{H} \right)^2 + a_5 \left(\frac{h_i}{H} \right)^3 \quad (9)$$

$$S \geq 1, i = 2 \text{ to } N + 1$$

where i is the story number; H_{vi} are the peak floor velocity correction factors for v_i^{si} ; T_1 is the fundamental period of the building; S is the strength ratio of the building (refer to Equation 4); and h_i/H is the ratio of the height of floor i over the total height of the building. Two separate regression analyses are performed for each framing system considering different building heights, one for 3- and 6-story buildings (with a_5 set to 0) and another for 12- and 16-story buildings.

Total floor velocity at Floor i , v_i^{si} , is computed following the simplified FEMA P-58 procedure:

$$v_i^{si} = PGV + \frac{T_1}{2\pi} \left(\frac{V_{y1}}{\frac{W_1}{g}} \Gamma_1 \right) \left(\frac{\Delta_i^{si}}{\delta_r^{si}} \right) * 0.3 \quad (10)$$

where PGV is peak ground velocity; T_1 is the fundamental period of the building; W_1 is the first modal weight of the building which cannot be less than 80% of the total weight, W ; V_{y1} is the yield strength of the building estimated by pushover analysis considering the first mode distribution of seismic forces; Γ_1 is the first mode participation factor; Δ_i^{si} is the story drift at story i estimated by the simplified procedure before correction (refer to the previous section); and δ_r^{si} is roof displacement with respect to the base of the building estimated by the simplified procedure before correction.

Table 2 presents regression coefficients a_0 through a_5 for estimating peak floor velocity, v_i^{si*} , for 3- and 6-story buildings and Table 3 presents the regression coefficients for 12- and 16-story buildings. Figures 13 through 16 show velocity ratios v_i^{si}/v_i^{in} for the 3-, 6-, 12-, and 16-story buildings, respectively. The presented results demonstrate significant differences between the peak floor velocities estimated by response-history analysis and those estimated by the simplified procedure before correction. To demonstrate the effectiveness of the regression model utilized in this study the corrected peak floor velocities, v_i^{si*} , were computed for all models and all ground motions and the velocity ratios v_i^{si*}/v_i^{in} are presented in Figures 20 through 23. Most of the median values of v_i^{si}/v_i^{in} are significantly improved by correcting the floor velocities by utilizing the correction factor H_{vi} .

Correction factors for estimating peak floor acceleration compliant with the simplified analysis procedure of FEMA P-58

Within the simplified analysis procedure of FEMA P-58, the floor accelerations are calculated by correcting the total floor acceleration at Floor i , a_i^{si} , with a correction factor H_{ai} following Equation 11. Peak ground acceleration was adopted as the baseline acceleration estimate for peak floor acceleration (Equation 12) based on FEMA P-58.

$$a_i^{si*} = H_{ai} * a_i^{si} \quad i = 2 \text{ to } N + 1 \quad (11)$$

$$a_i^{si} = PGA \quad i = 2 \text{ to } N + 1 \quad (12)$$

To develop correction factors H_{ai} for a_i^{si} , residual values, $\ln(a_i^{si}/a_i^{in})$, were generated for all models, stories, ground motions and considered seismic intensities. Only the values associated with S smaller than 10 and/or μ smaller than 6 for BRBF and/or μ smaller than 8 for SCBF were included in the regression analysis. The following regression model was used to develop corrections factors for a_i^{si} :

$$\ln H_{ai} = a_0 + a_1 T_1 + a_2 S + a_3 \frac{h_i}{H} + a_4 \left(\frac{h_i}{H}\right)^2 + a_5 \left(\frac{h_i}{H}\right)^3 \quad (13)$$

$$S \geq 1, i = 2 \text{ to } N + 1$$

where i is the story number; H_{ai} are the peak floor acceleration correction factors for a_i^{si} ; T_1 is the fundamental period of the building; S is the strength ratio of the building (refer to Equation 4); and h_i/H is the ratio of the height of floor i over the total height of the building. Two separate regression analyses are performed for each framing system considering different building heights, one for 3- and 6-story buildings (with a_5 set to 0) and another for 12- and 16-story buildings.

Table 2 presents regression coefficients a_0 through a_5 for estimating peak floor acceleration, a_i^{si*} , for 3- and 6-story buildings and Table 3 presents the regression coefficients for 12- and 16-story buildings. Figures 24 through 27 show acceleration ratios a_i^{si}/a_i^{in} for the 3-, 6-, 12-, and 16-story buildings, respectively. The presented results demonstrate significant differences between the peak floor velocities estimated by response-history analysis and those estimated by the simplified procedure before correction. To demonstrate the effectiveness of the regression model utilized in this study the corrected peak floor accelerations, a_i^{si*} , were computed for all models and all ground motions and the acceleration ratios a_i^{si*}/a_i^{in} are presented in Figures 31 through 34. Most of the median values of a_i^{si}/a_i^{in} are significantly improved by correcting the floor velocities by utilizing the correction factors H_{ai} .

References

- Huang, Y., Whittaker, A. S., Luco, N., and Hamburger, R. O. (2011). "Scaling earthquake ground motions for performance-based assessment of buildings." *Journal of Structural Engineering*, 137(3), 311-321.
- Huang, Y., & Whittaker, A. (2012). *Simplified Analysis Procedures for Next-generation Performance-based Seismic Design*. Applied Technology Council, Redwood City, CA.
- Federal Emergency Management Agency (FEMA). (2012). FEMA P-58: *Seismic performance assessment of buildings, volume 1—methodology*. Federal Emergency Management Agency, Washington, DC.
- Chen, C., & Mahin, S. A. (2012). *Performance-Based Seismic Demand Assessment of Concentrically Braced Steel Frame Buildings*. Pacific Earthquake Engineering Research Center, Berkeley, CA.

Table 1: Notations and fundamental periods of the buildings analyzed in the study.

Notation	Fundamental period T_1 (sec)	No. of stories	Lateral force resisting system
M1	.58	3	Special Concentrically Braced Frame (3SCBFDmax)
M2	.8		Special Concentrically Braced Frame (3SCBFDmin)
M3	.8		Buckling Restrained Braced Frame (3BRBFDmax)
M4	1.27		Buckling Restrained Braced Frame (3BRBFDmin)
M5	1.02	6	Special Concentrically Braced Frame (6SCBFDmax)
M6	1.51		Special Concentrically Braced Frame (6SCBFDmin)
M7	1.37		Buckling Restrained Braced Frame (6BRBFDmax)
M8	2.43		Buckling Restrained Braced Frame (6BRBFDmin)
M9	1.91	12	Special Concentrically Braced Frame (12SCBFDmax)
M10	2.64		Special Concentrically Braced Frame (12SCBFDmin)
M11	2.89		Buckling Restrained Braced Frame (12BRBFDmax)
M12	3.63		Buckling Restrained Braced Frame (12BRBFDmin)
M13	3.16	16	Special Concentrically Braced Frame (16SCBFDmax)
M14	4.67		Special Concentrically Braced Frame (16SCBFDmin)
M15	3.86		Buckling Restrained Braced Frame (16BRBFDmax)
M16	5.0		Buckling Restrained Braced Frame (16BRBFDmin)

Table 2: Coefficients for the story-drift, floor-velocity, and floor acceleration correction factors considering 3- and 6- story SCBF and BRBF buildings used in the study.

H	Frame Type	a_0	a_1	a_2	a_3	a_4
$H_{\Delta S}$	SCBF	0.753	0.181	-0.042	-2.449	1.929
$H_{\Delta B}$	BRBF	0.334	0.136	-0.059	-0.676	0.562
H_{vS}	SCBF	0.203	0.227	-0.074	-0.449	0.193
H_{vB}	BRBF	0.349	0.016	-0.066	0.508	.157
H_{aS}	SCBF	1.152	-0.469	-0.0387	-0.043	0.473
H_{aB}	BRBF	0.919	-0.295	-0.042	-0.247	0.426

Table 3: Coefficients for the story-drift, floor-velocity, and floor acceleration correction factors for the 12-,16- story buildings used in the study

H	Frame Type	a_0	a_1	a_2	a_3	a_4	a_5
$H_{\Delta S}$	SCBF	1.264	0.053	-0.0333	-6.932	10.623	-4.798
$H_{\Delta B}$	BRBF	1.106	0.135	-0.057	-5.456	7.376	-2.882
H_{vS}	SCBF	0.6	-0.112	-0.064	3.237	-6.686	4.452
H_{vB}	BRBF	0.8126	-0.10451	-0.092	2.38	-4.956	3.278
H_{aS}	SCBF	0.628	-0.172	-0.046	3.517	-8.506	5.533
H_{aB}	BRBF	0.929	-0.191	-0.057	1.667	-4.596	3.059

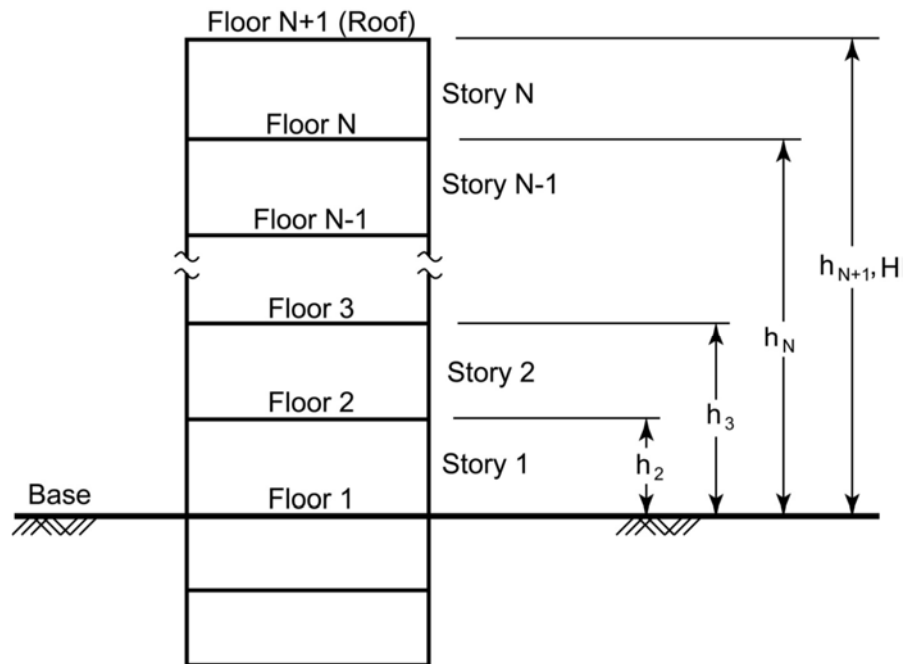


Figure 1. Notation of floor levels, story numbers, and floor heights.

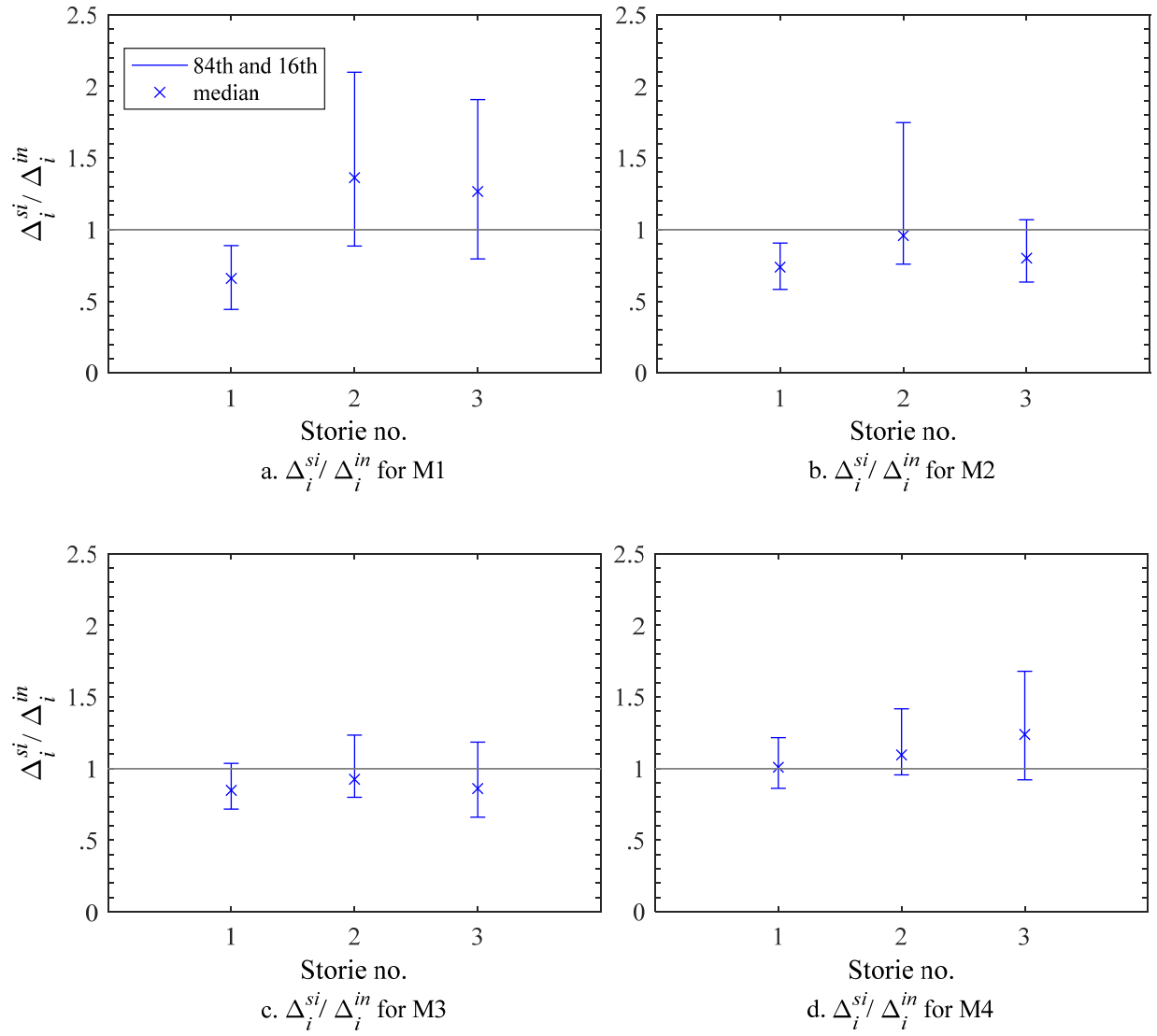
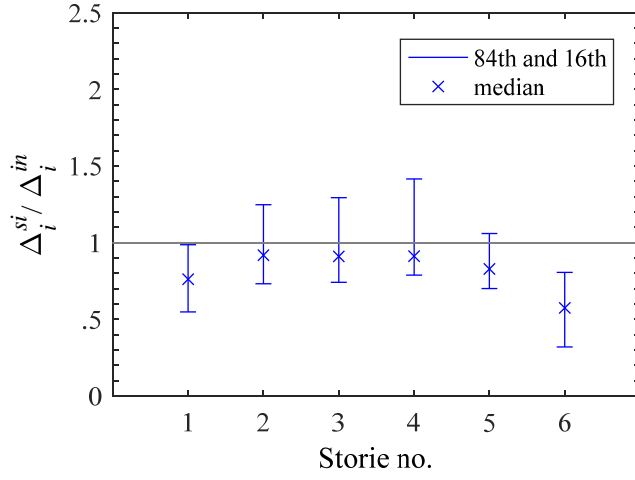
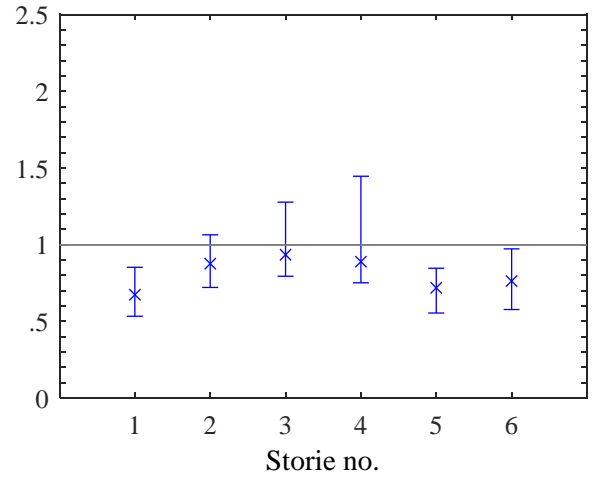


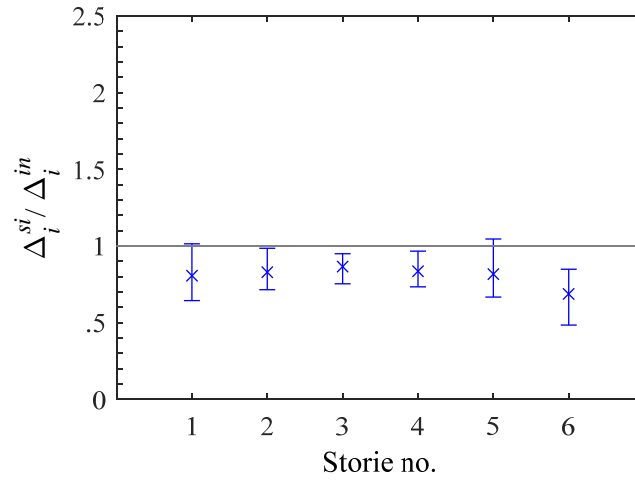
Figure 2. 84th, 50th, and 16th percentiles of $\Delta_i^{si} / \Delta_i^{in}$ for three-story models.



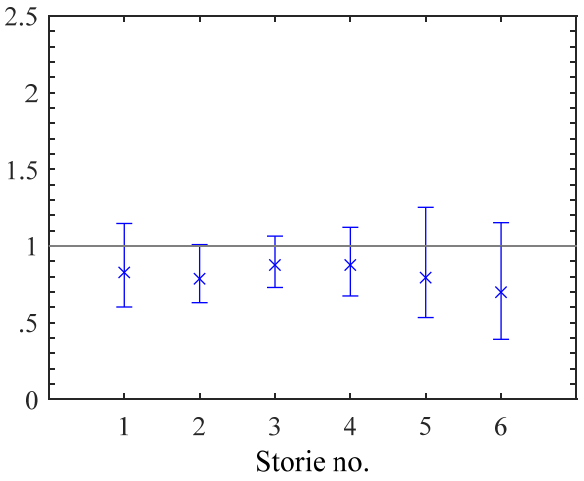
a. $\Delta_i^{si} / \Delta_i^{in}$ for M5



b. $\Delta_i^{si} / \Delta_i^{in}$ for M6



c. $\Delta_i^{si} / \Delta_i^{in}$ for M7



d. $\Delta_i^{si} / \Delta_i^{in}$ for M8

Figure 3. 84th, 50th, and 16th percentiles of $\Delta_i^{si} / \Delta_i^{in}$ for six-story models.

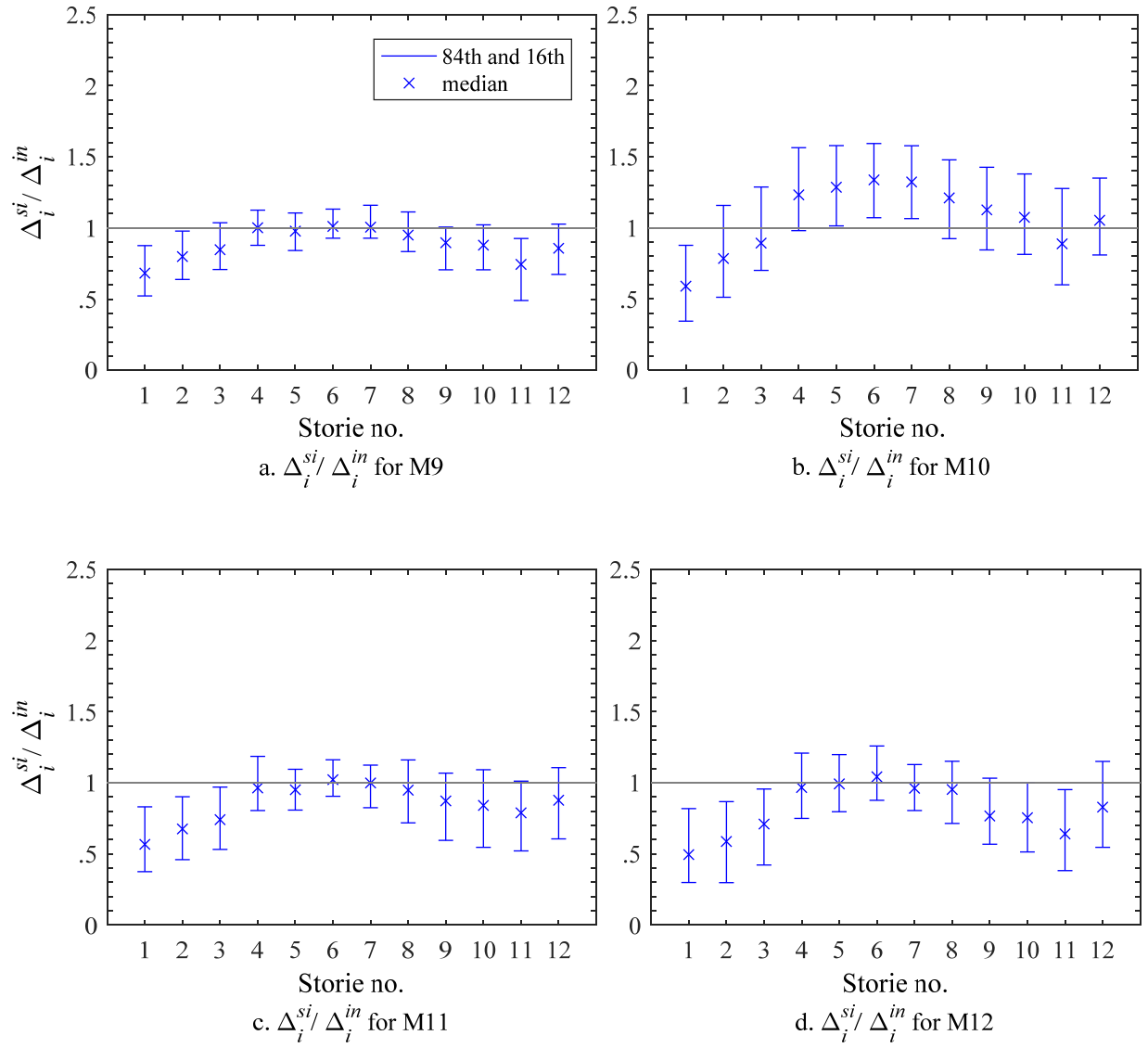


Figure 4. 84th, 50th, and 16th percentiles of $\Delta_i^{si} / \Delta_i^{in}$ for twelve-story models.

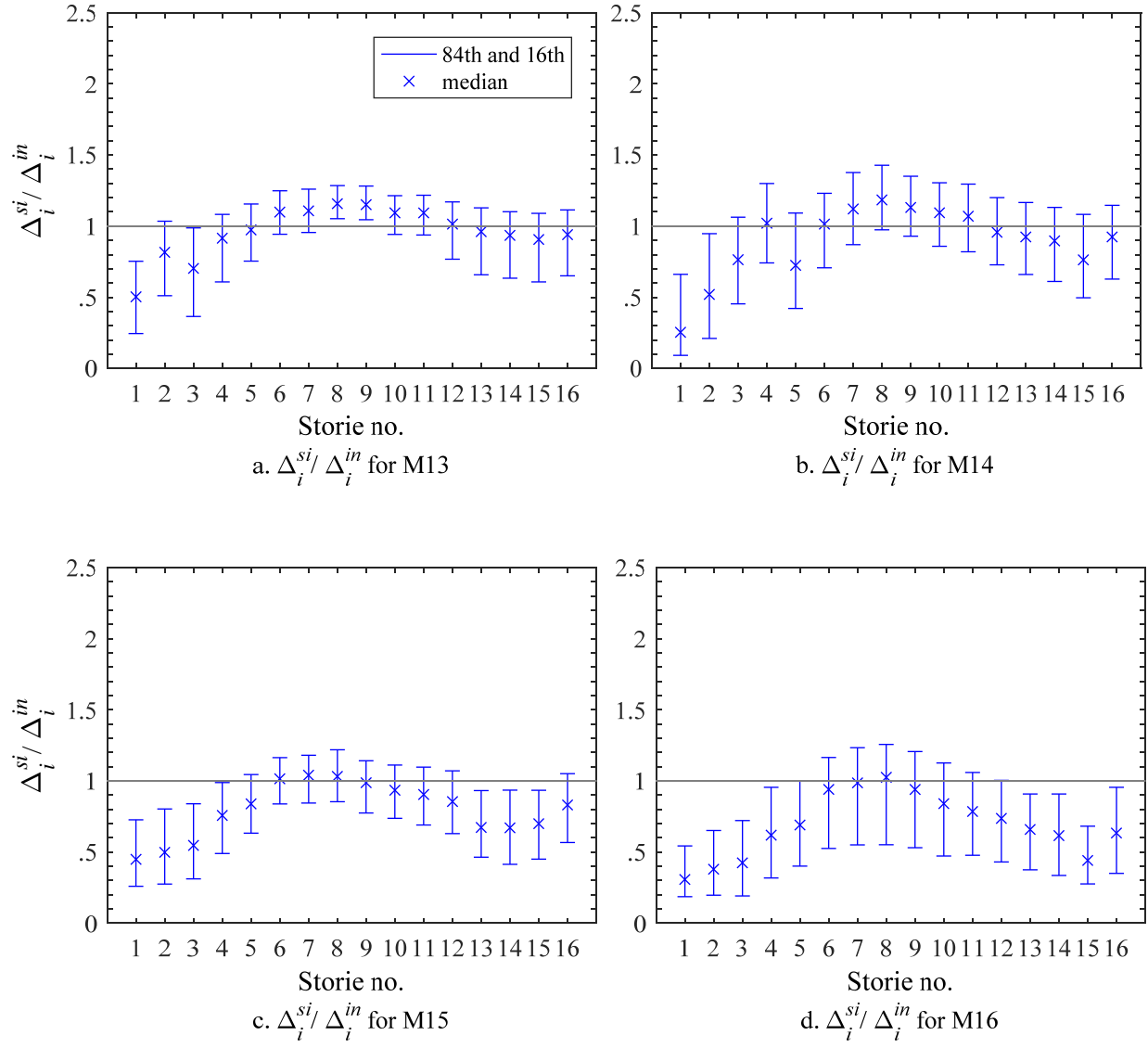


Figure 5. 84th, 50th, and 16th percentiles of $\Delta_i^{si} / \Delta_i^{in}$ for sixteen-story models.

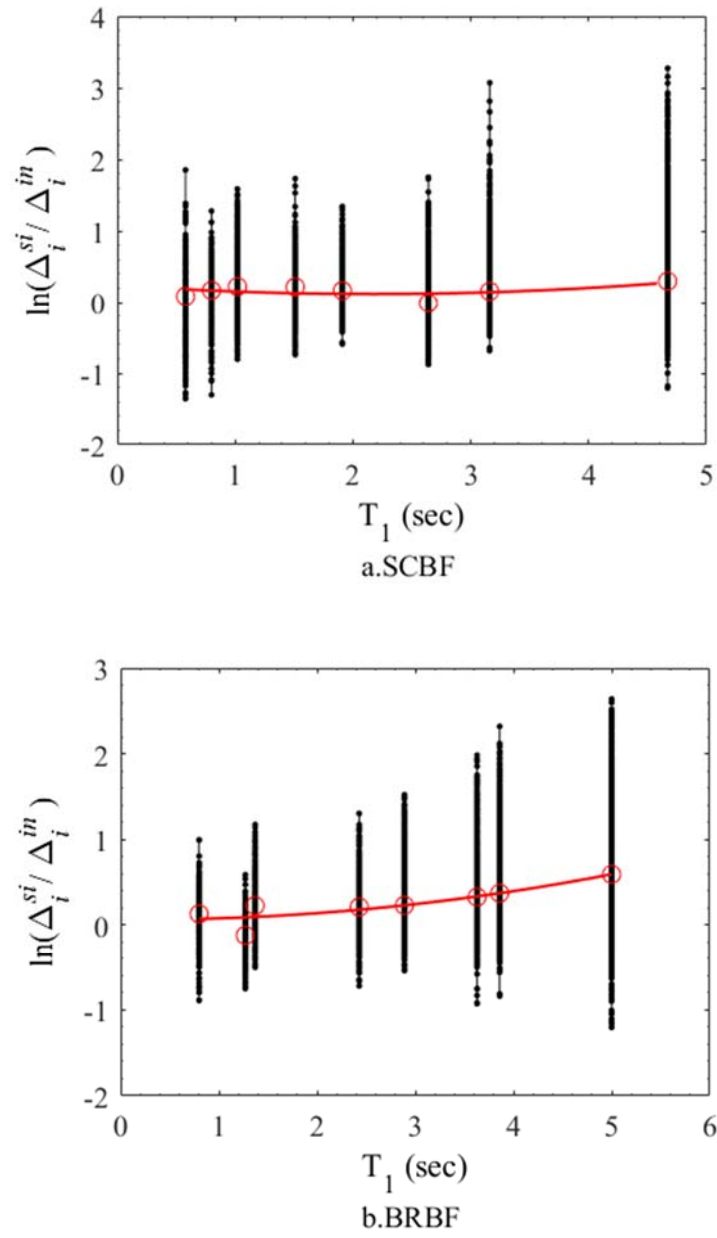


Figure 6. Inter-model residuals for $\Delta_i^{si} / \Delta_i^{in}$ as a function of T_1 and framing type.

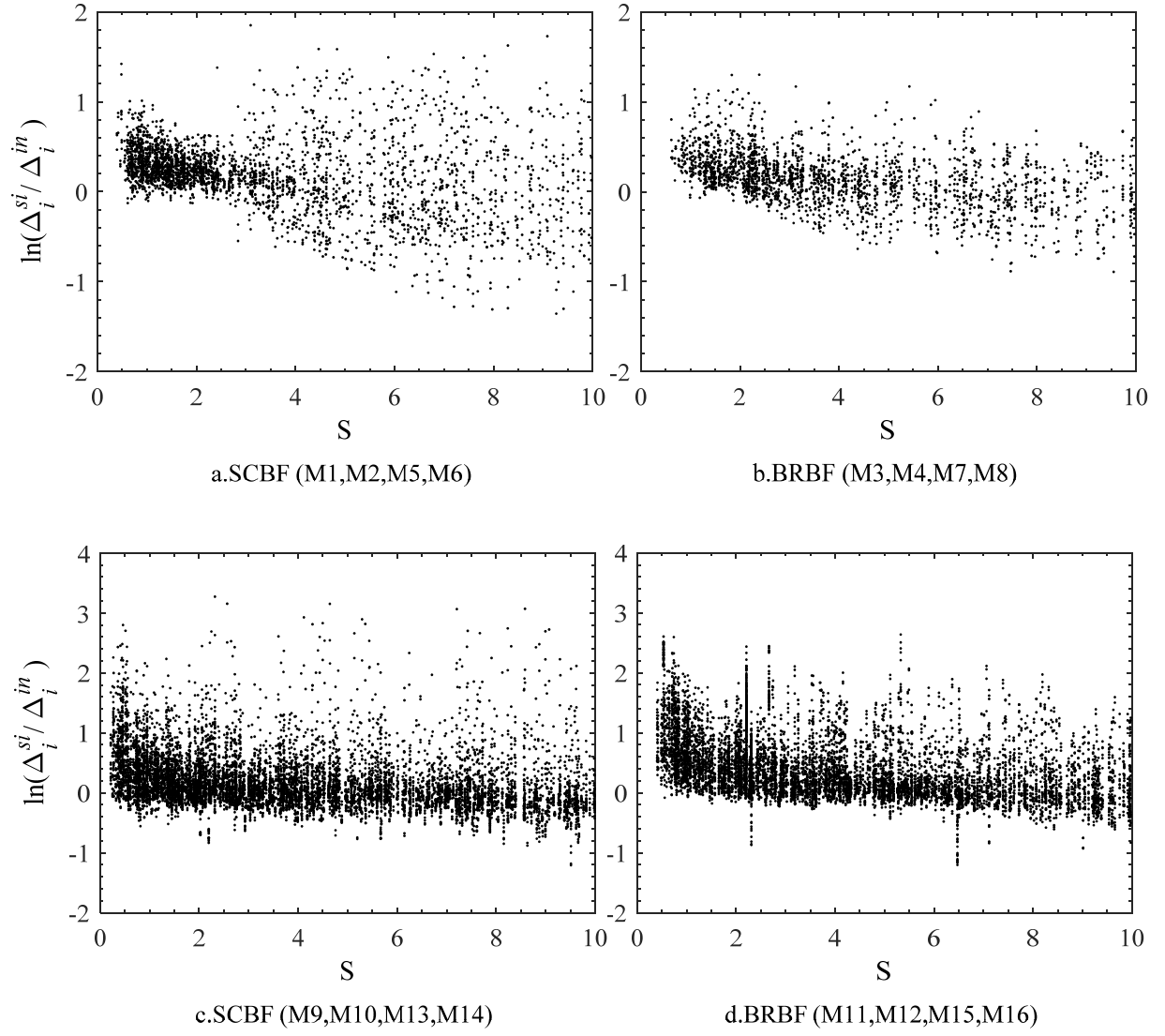


Figure 7. $\Delta_i^{si}/\Delta_i^{in}$ as a function of S and framing type.

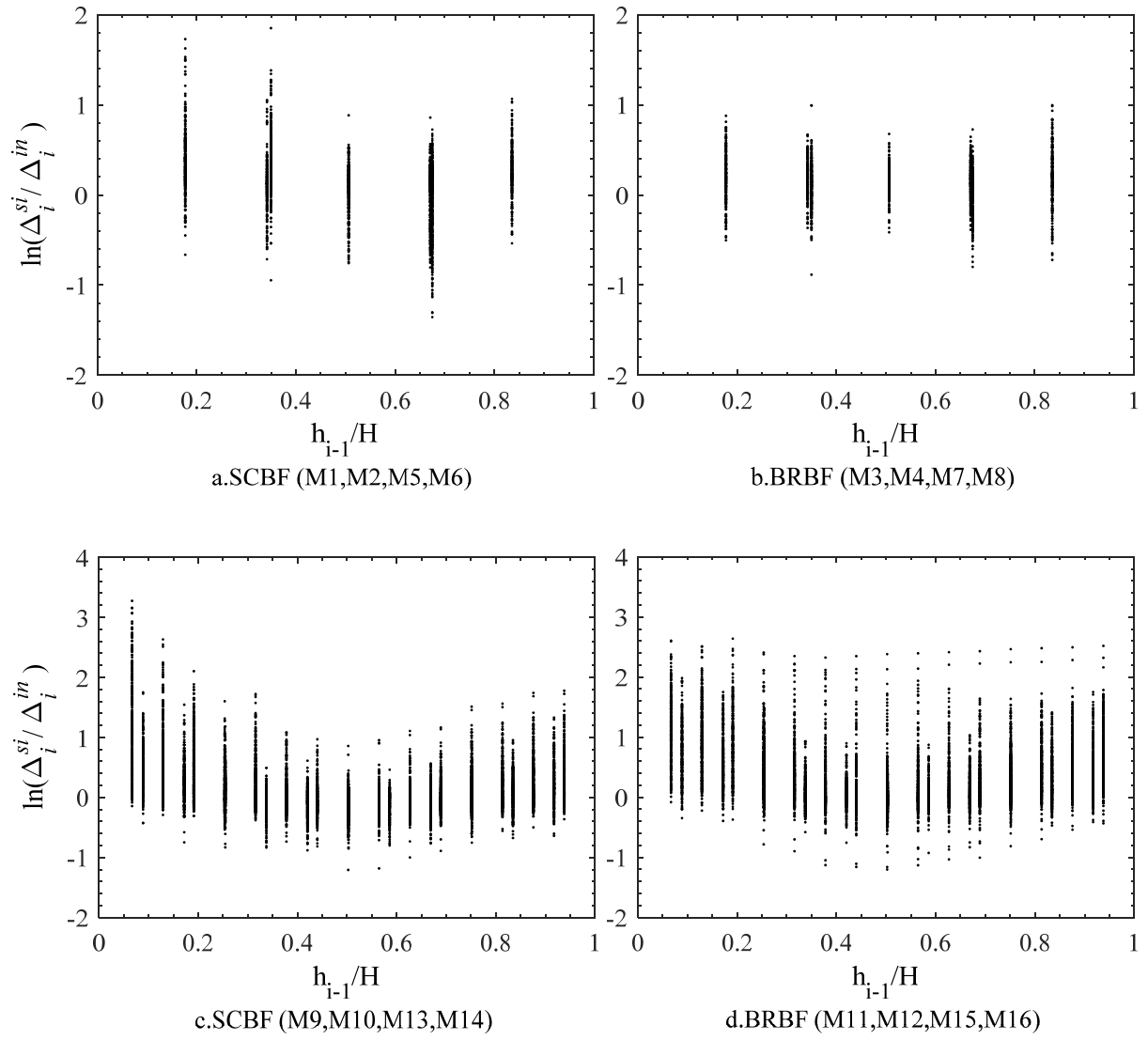


Figure 8. $\Delta_i^{sj}/\Delta_i^{in}$ as a function of h_i/H and framing type.

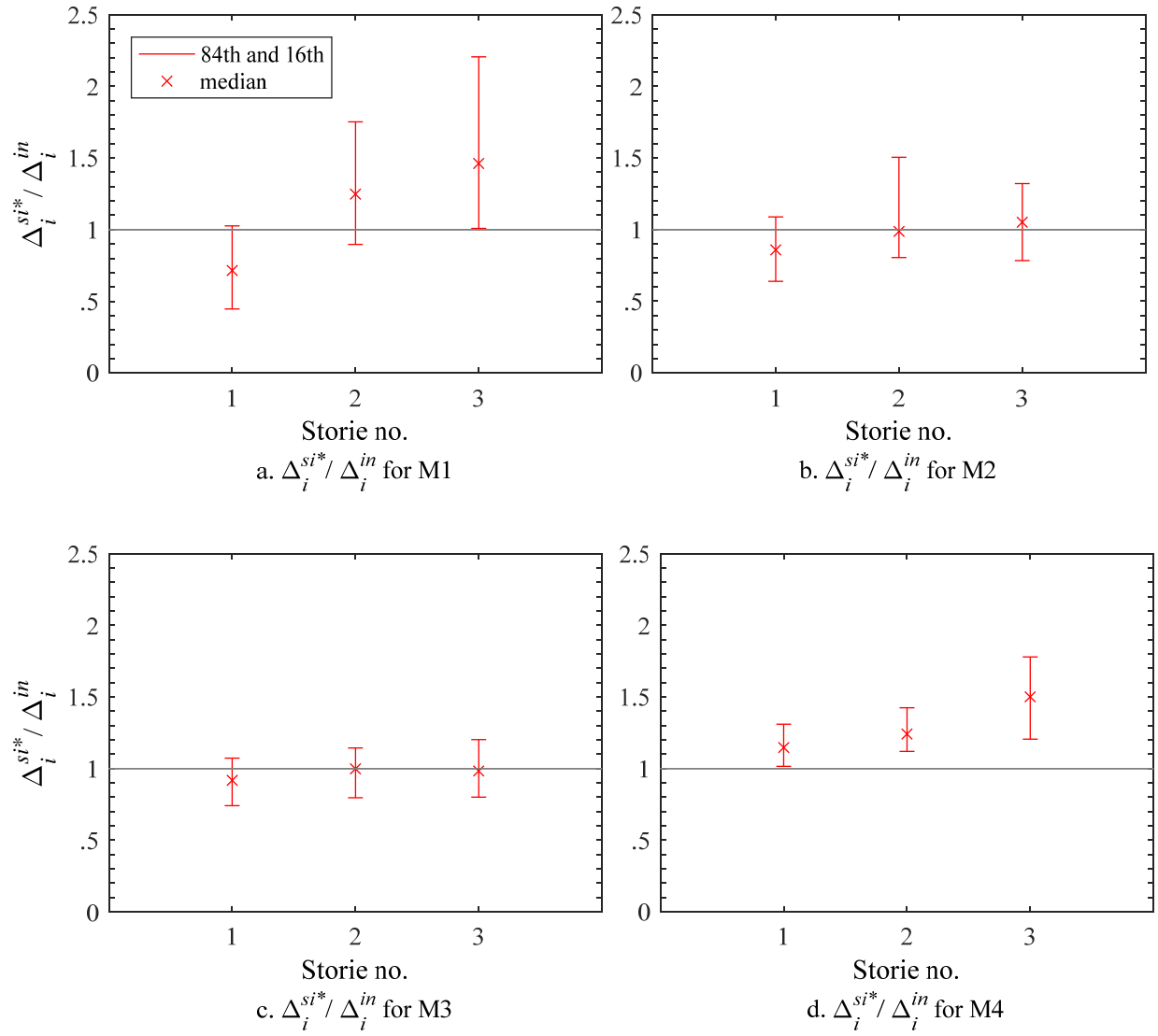


Figure 9. 84th, 50th, and 16th percentiles of $\Delta_i^{si*} / \Delta_i^{in}$ for three-story models.

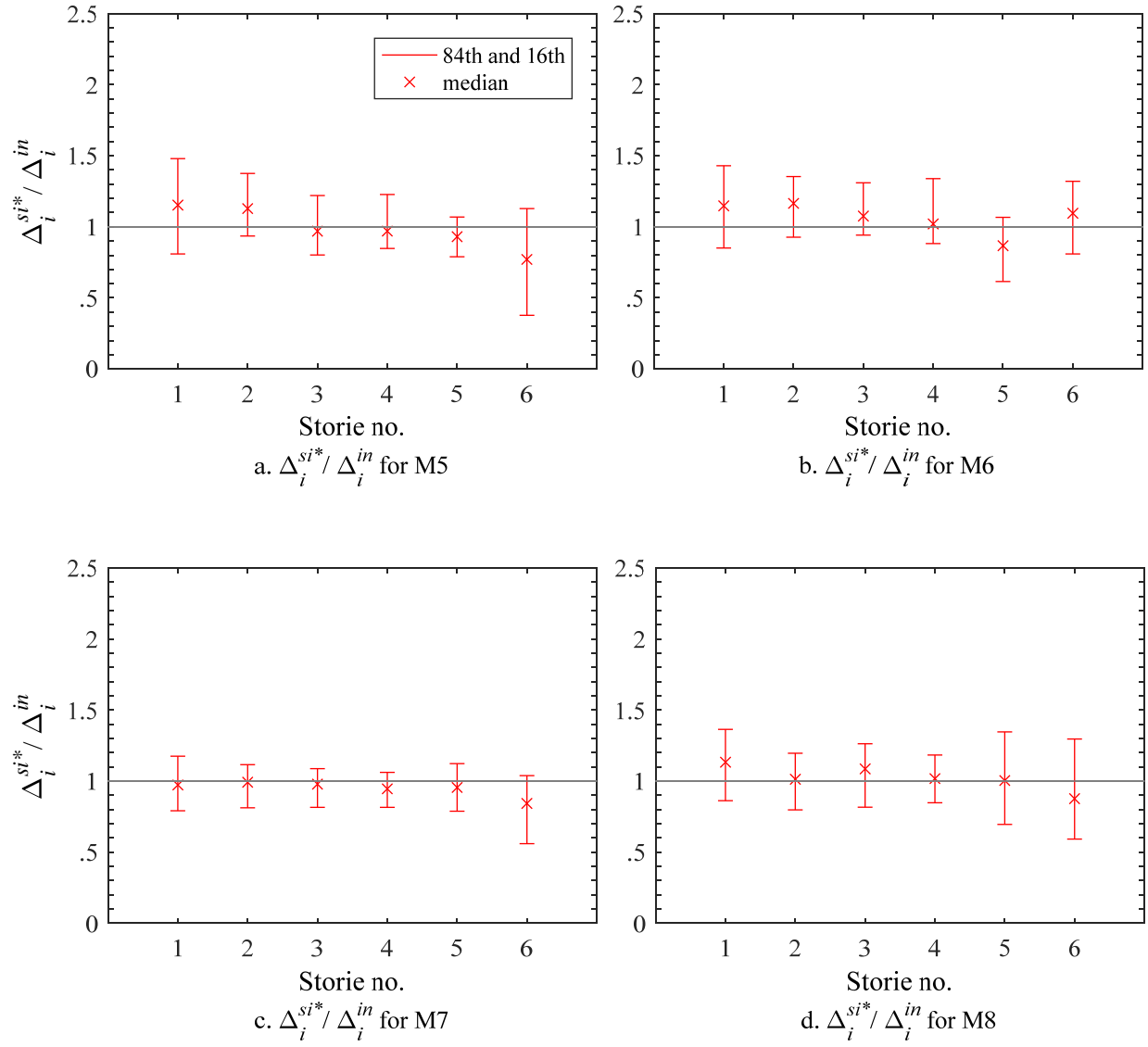


Figure 10. 84th, 50th, and 16th percentiles of $\Delta_i^{si*} / \Delta_i^{in}$ for six-story models.

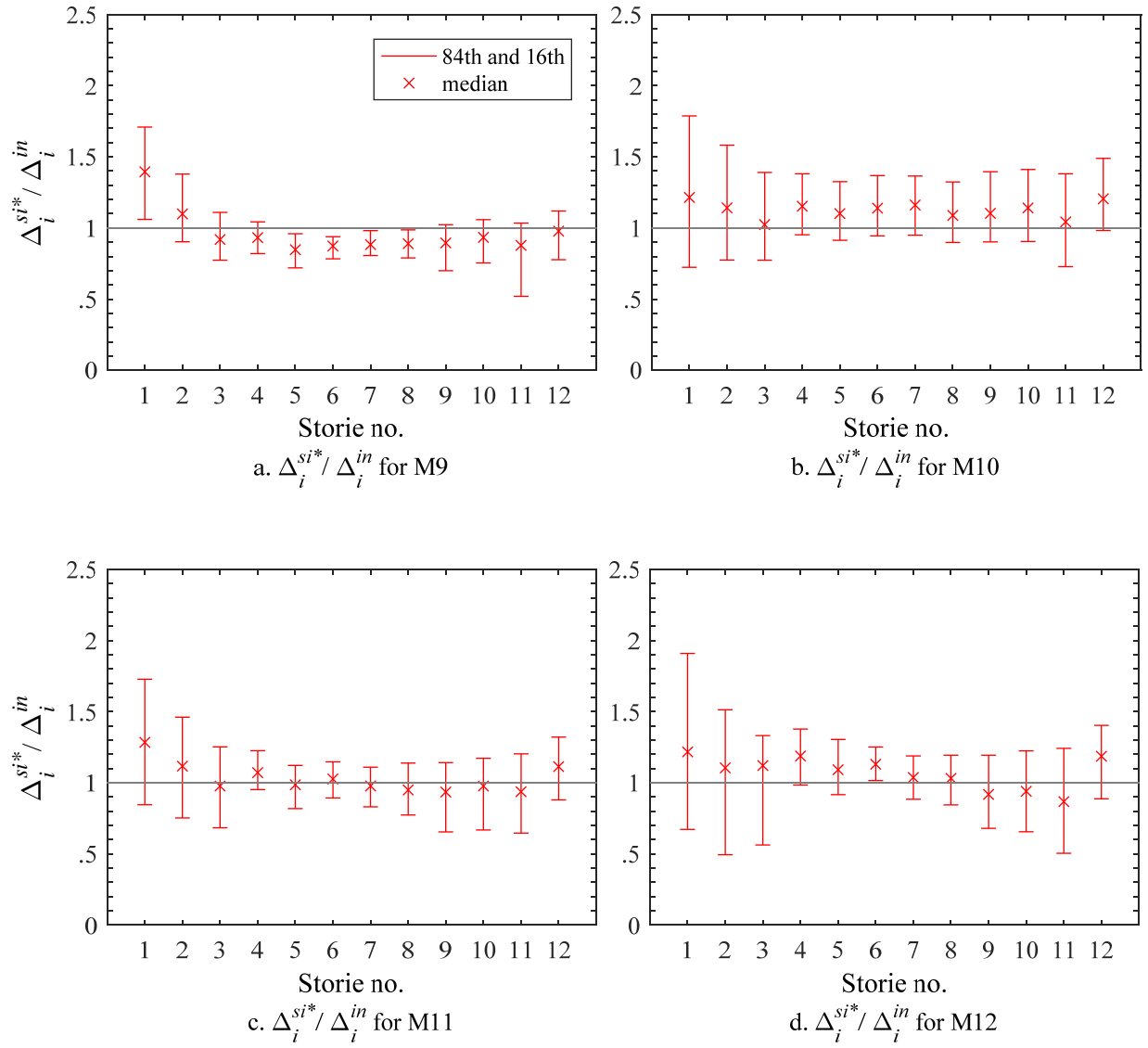


Figure 11. 84th, 50th, and 16th percentiles of $\Delta_i^{si*} / \Delta_i^{in}$ for twelve-story models.

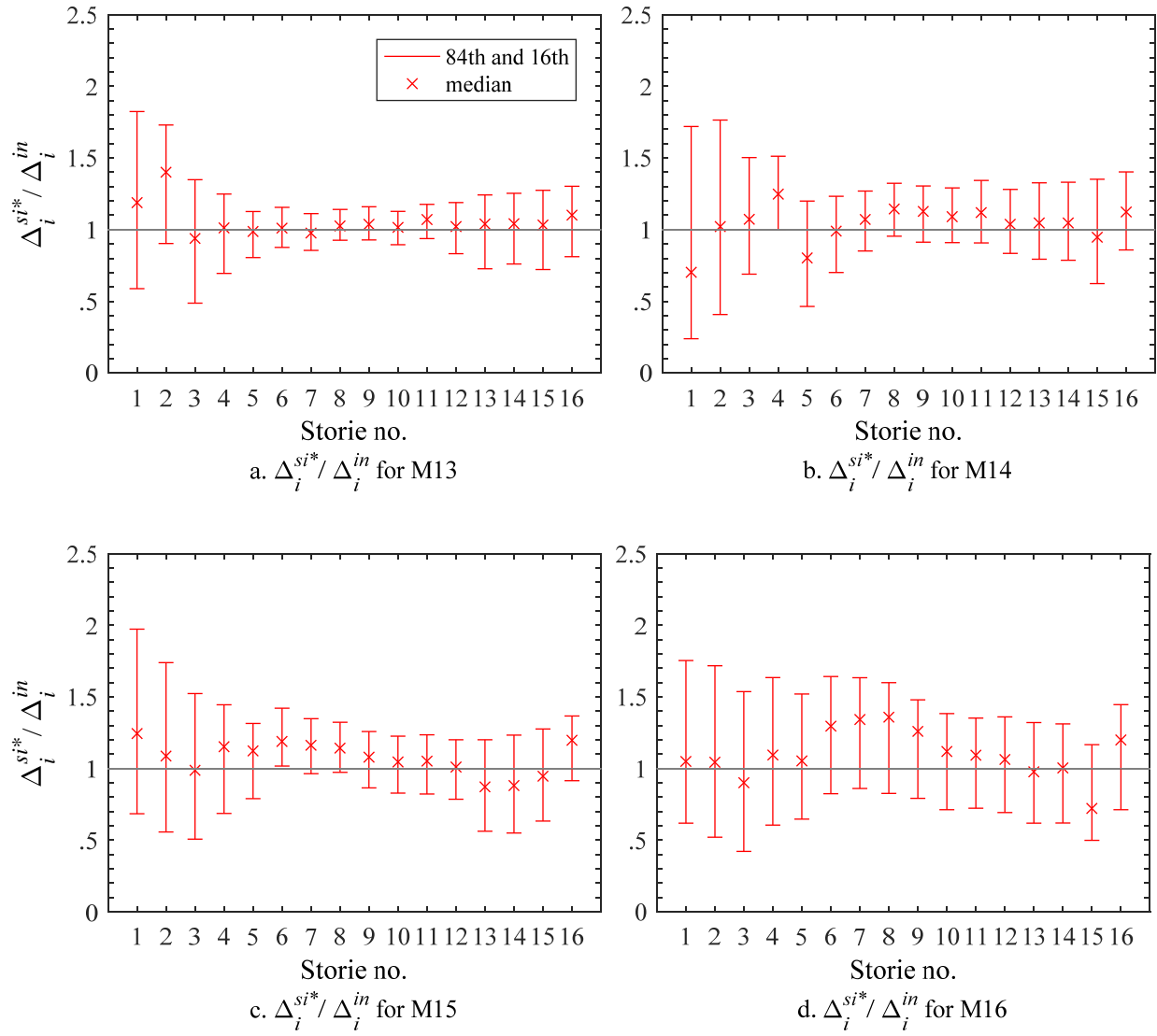


Figure 12. 84th, 50th, and 16th percentiles of $\Delta_i^{si*} / \Delta_i^{in}$ for sixteen-story models.

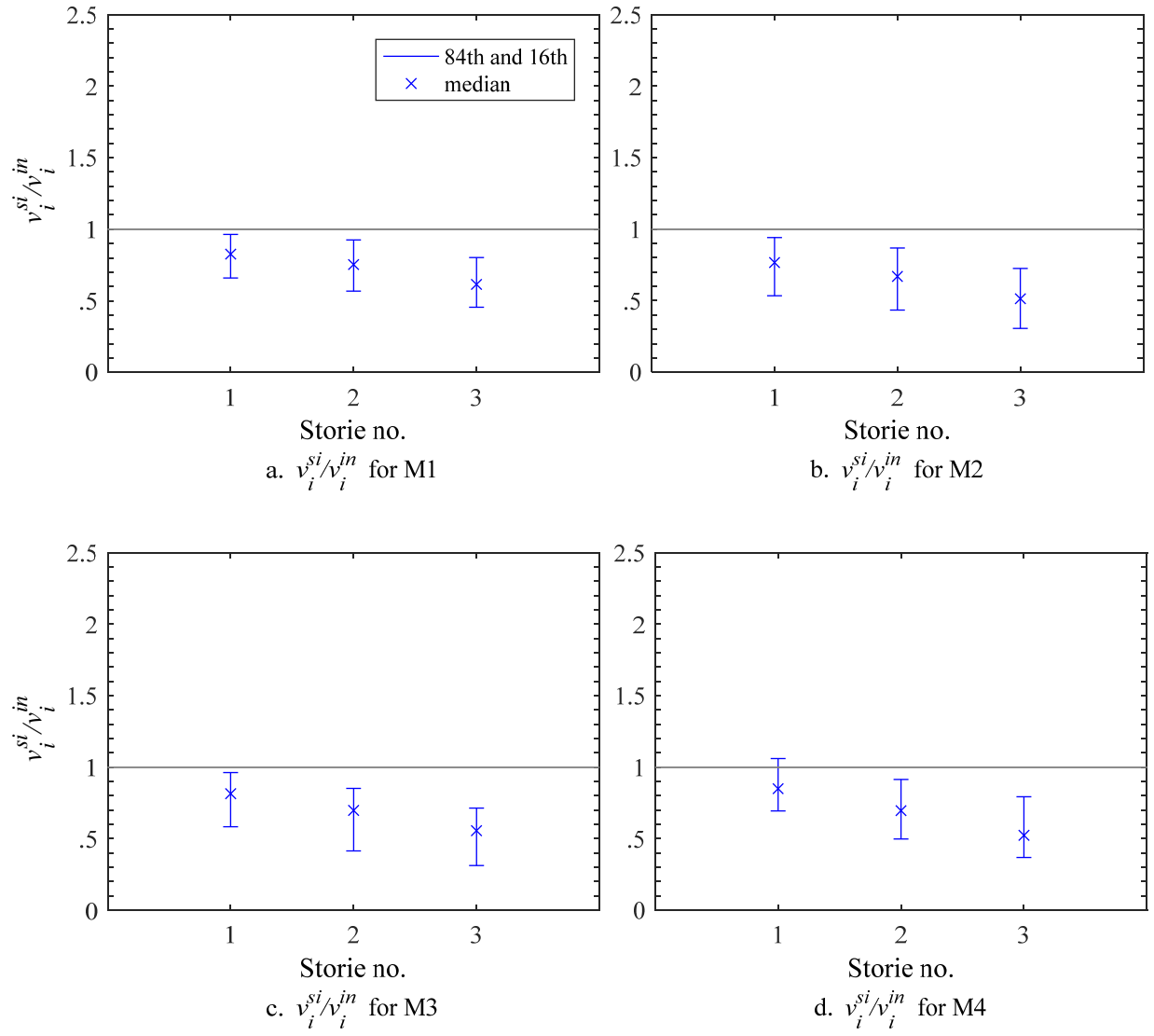


Figure 13. 84th, 50th, and 16th percentiles of v_i^{si}/v_i^{ni} for three-story models.

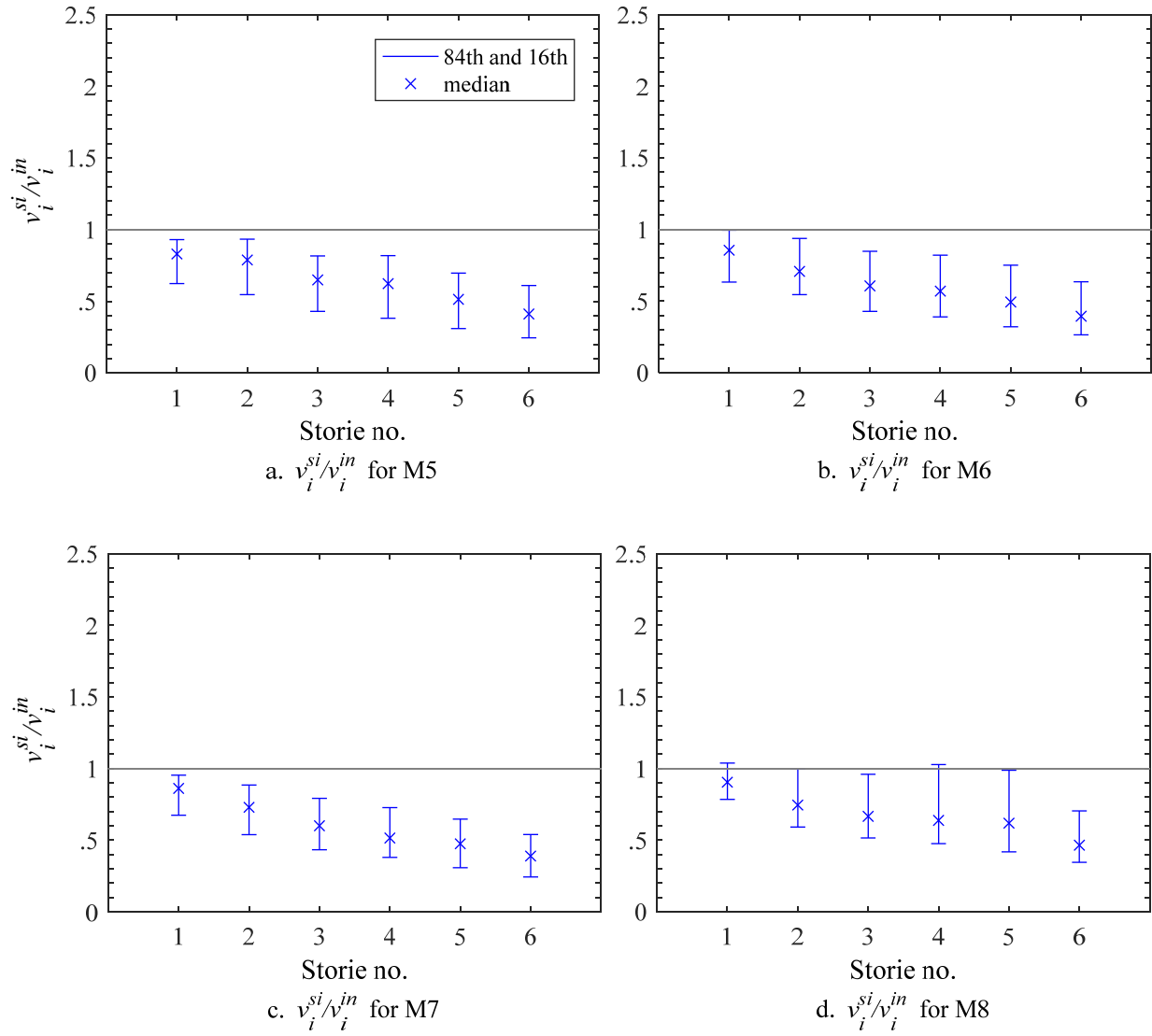


Figure 14. 84th, 50th, and 16th percentiles of v_i^{si}/v_i^{ni} for six-story models.

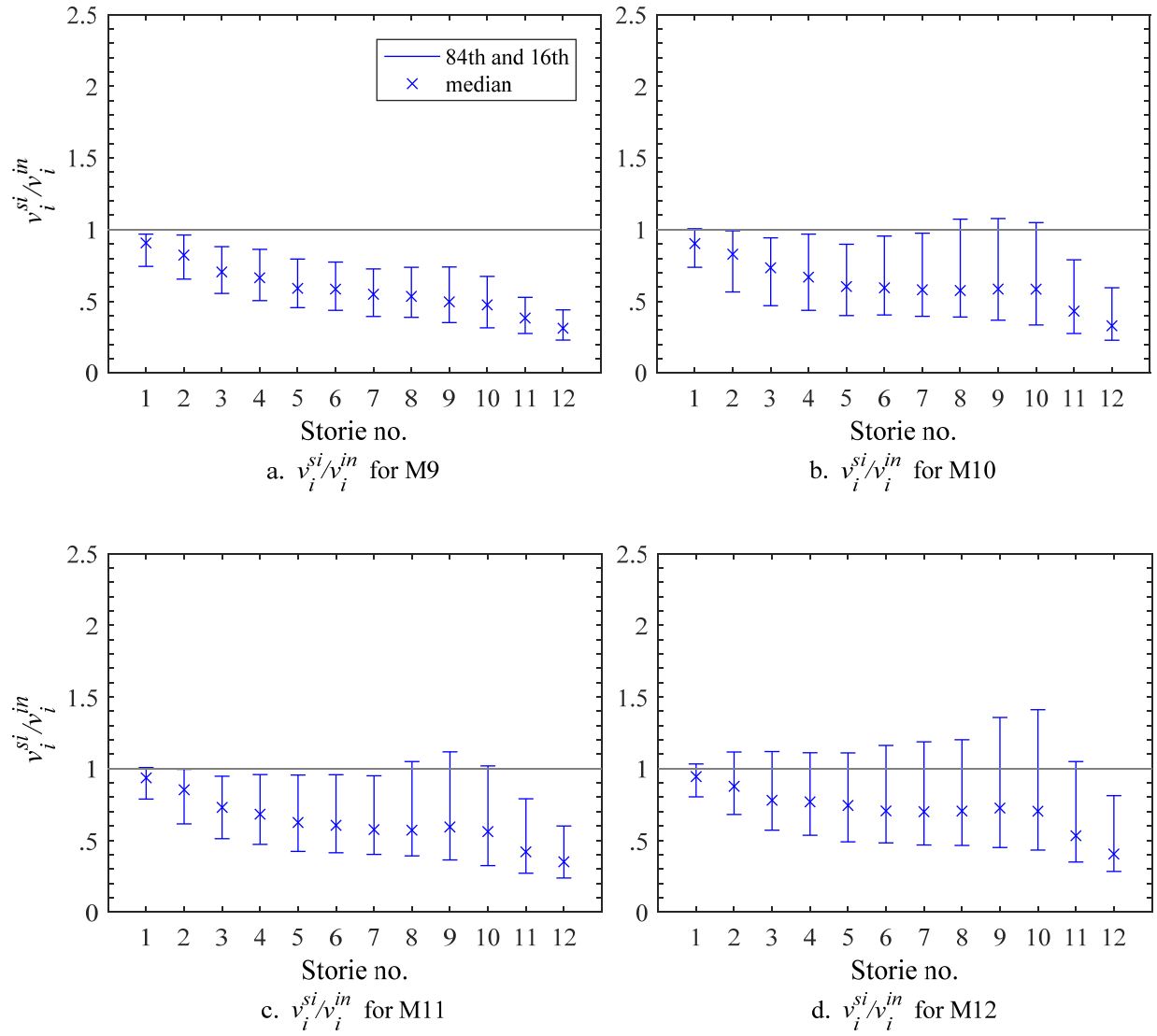
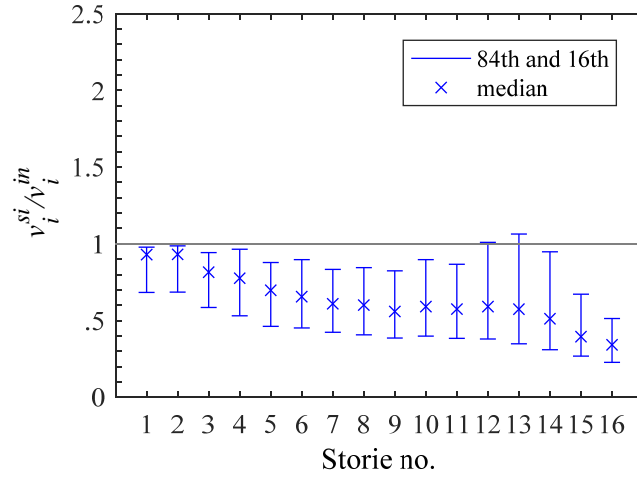
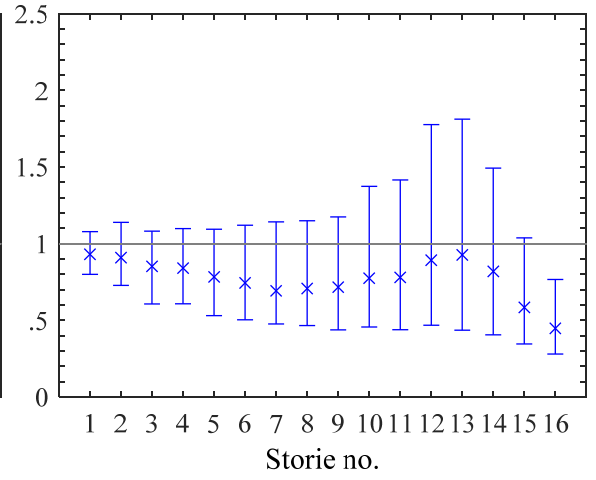


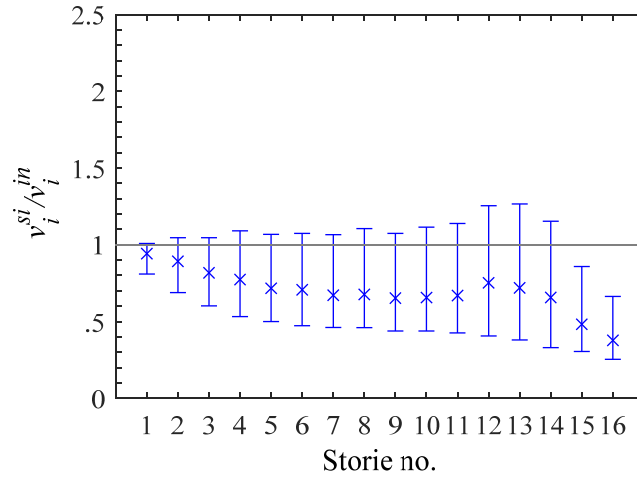
Figure 15. 84th, 50th, and 16th percentiles of v_i^{si}/v_i^{ni} for twelve-story models.



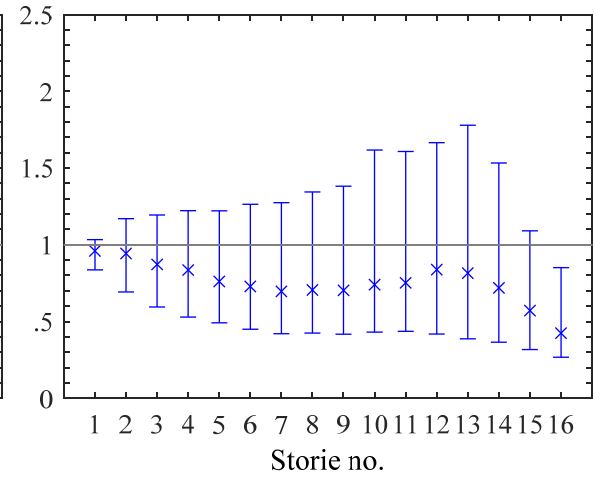
a. v_i^{si}/v_i^{in} for M13



b. v_i^{si}/v_i^{in} for M14



c. v_i^{si}/v_i^{in} for M15



d. v_i^{si}/v_i^{in} for M16

Figure 16. 84th, 50th, and 16th percentiles of v_i^{si}/v_i^{ni} for sixteen-story model.

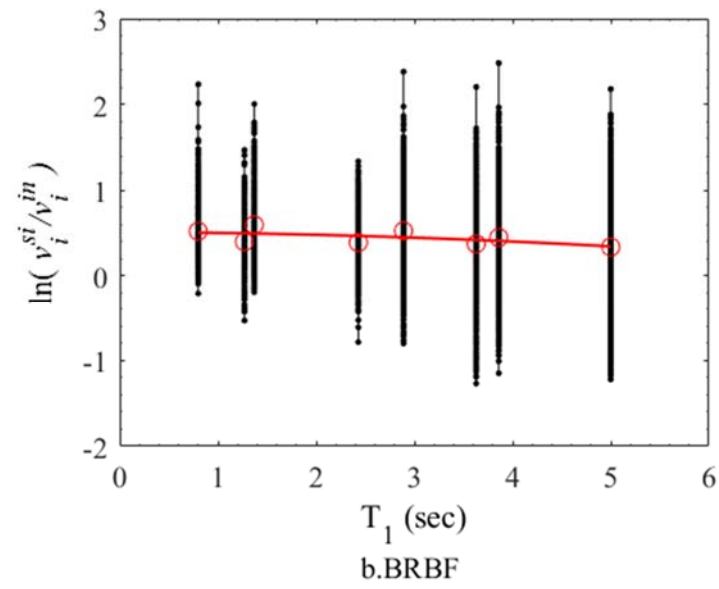
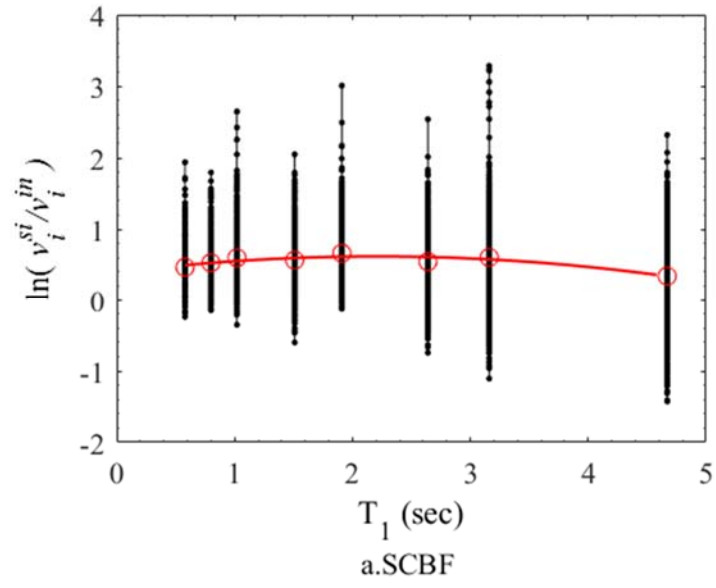


Figure 17. Inter-model residuals for v_i^{si}/v_i^{ni} as a function of T_1 and framing type.

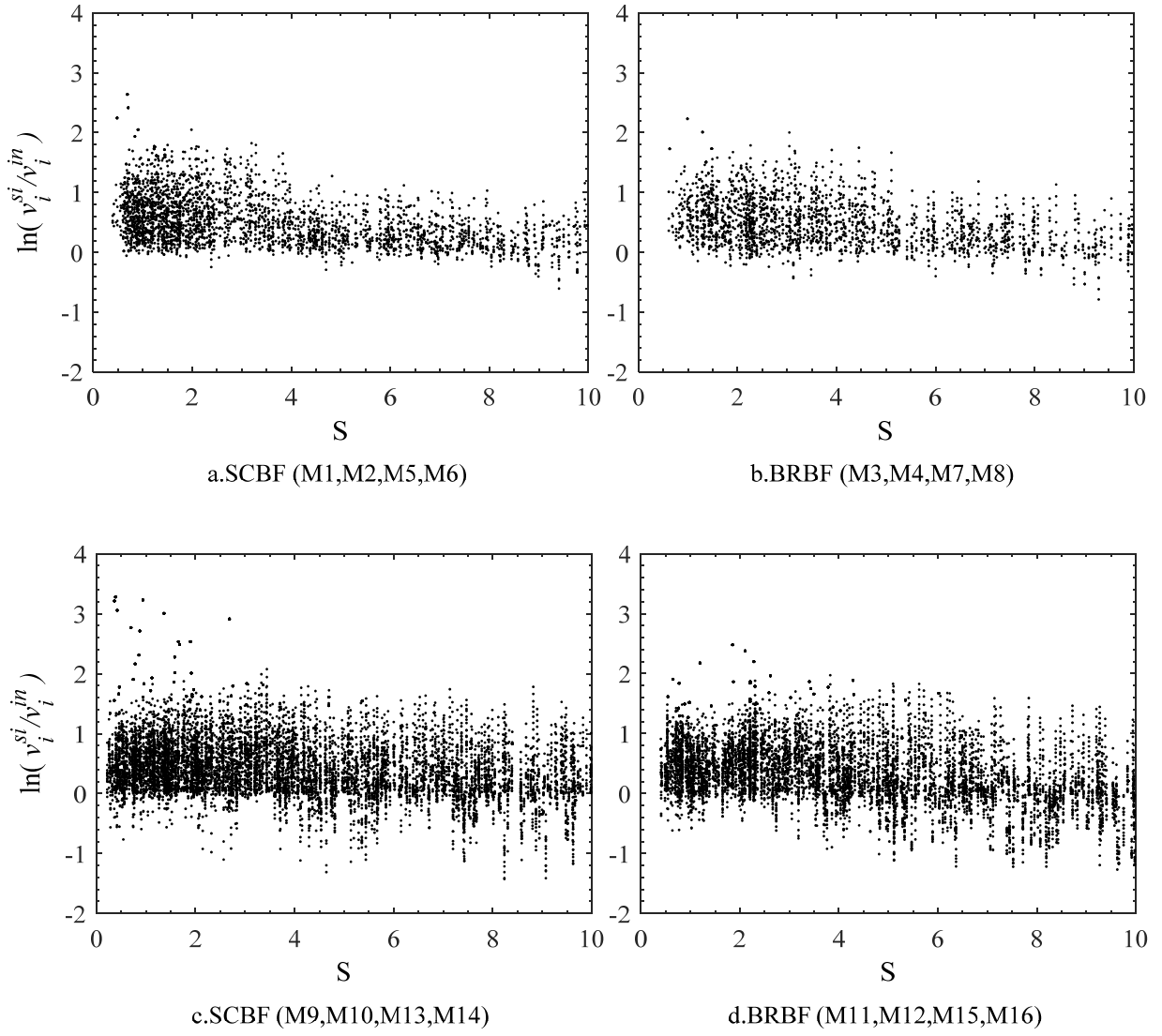


Figure 18. v_i^{sl}/v_i^{in} as a function of S and framing type.

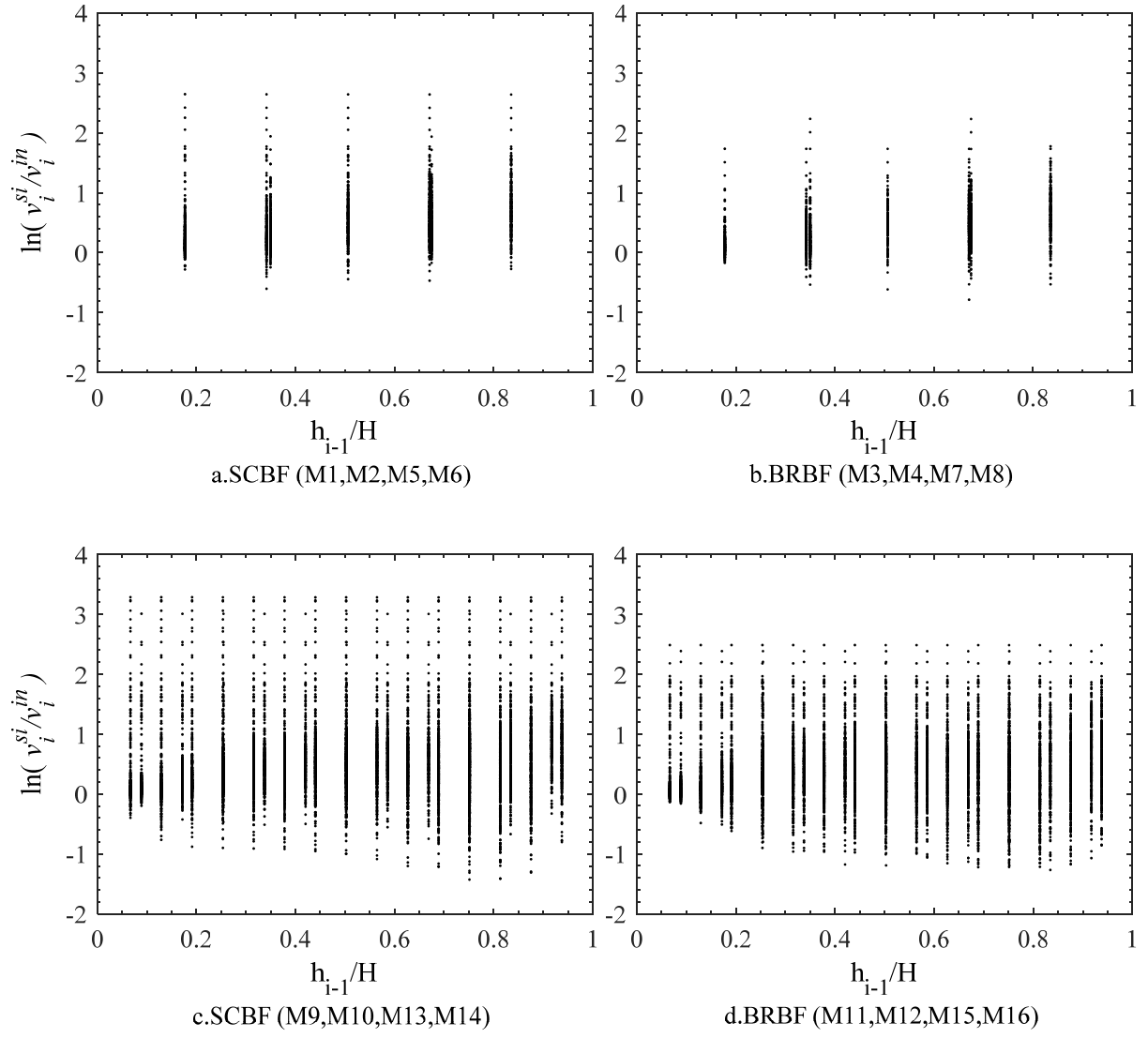


Figure 19. v_i^{si}/v_i^{ni} as a function of h_i/H and framing type.

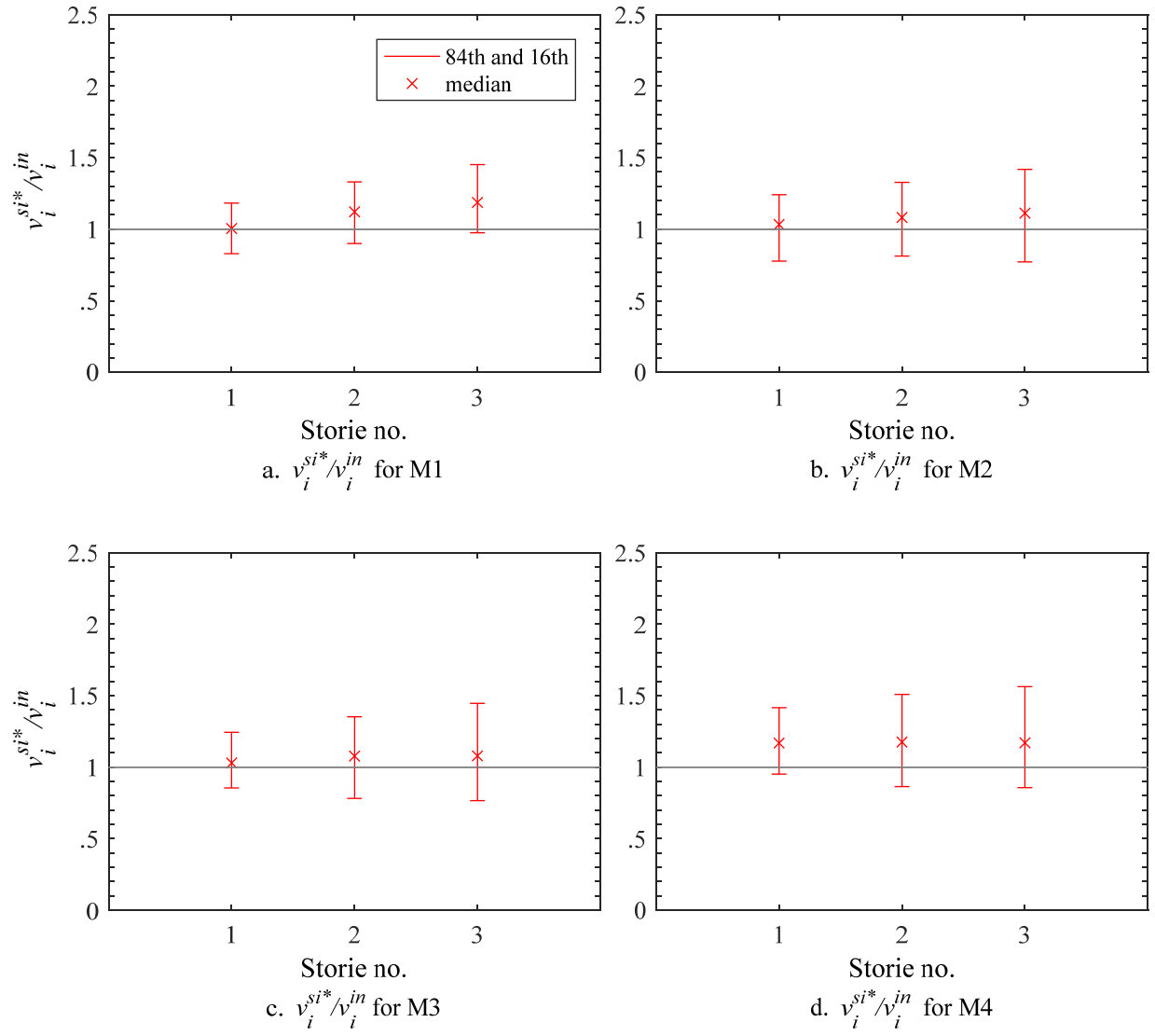


Figure 20. 84th, 50th, and 16th percentiles of v_i^{si*}/v_i^{ni} for three-story models.

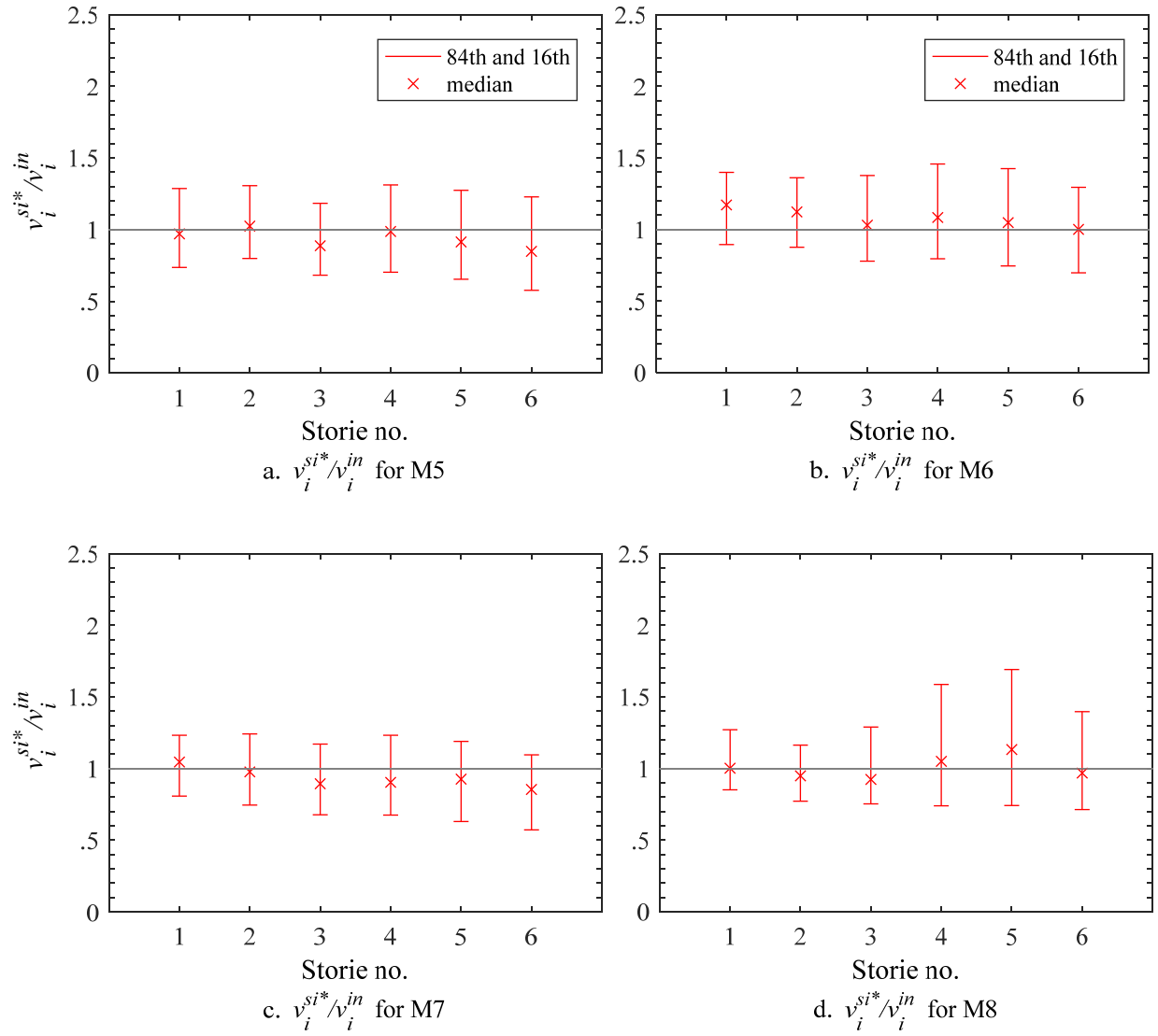


Figure 21. 84th, 50th, and 16th percentiles of v_i^{si*}/v_i^{ni} for six-story models.

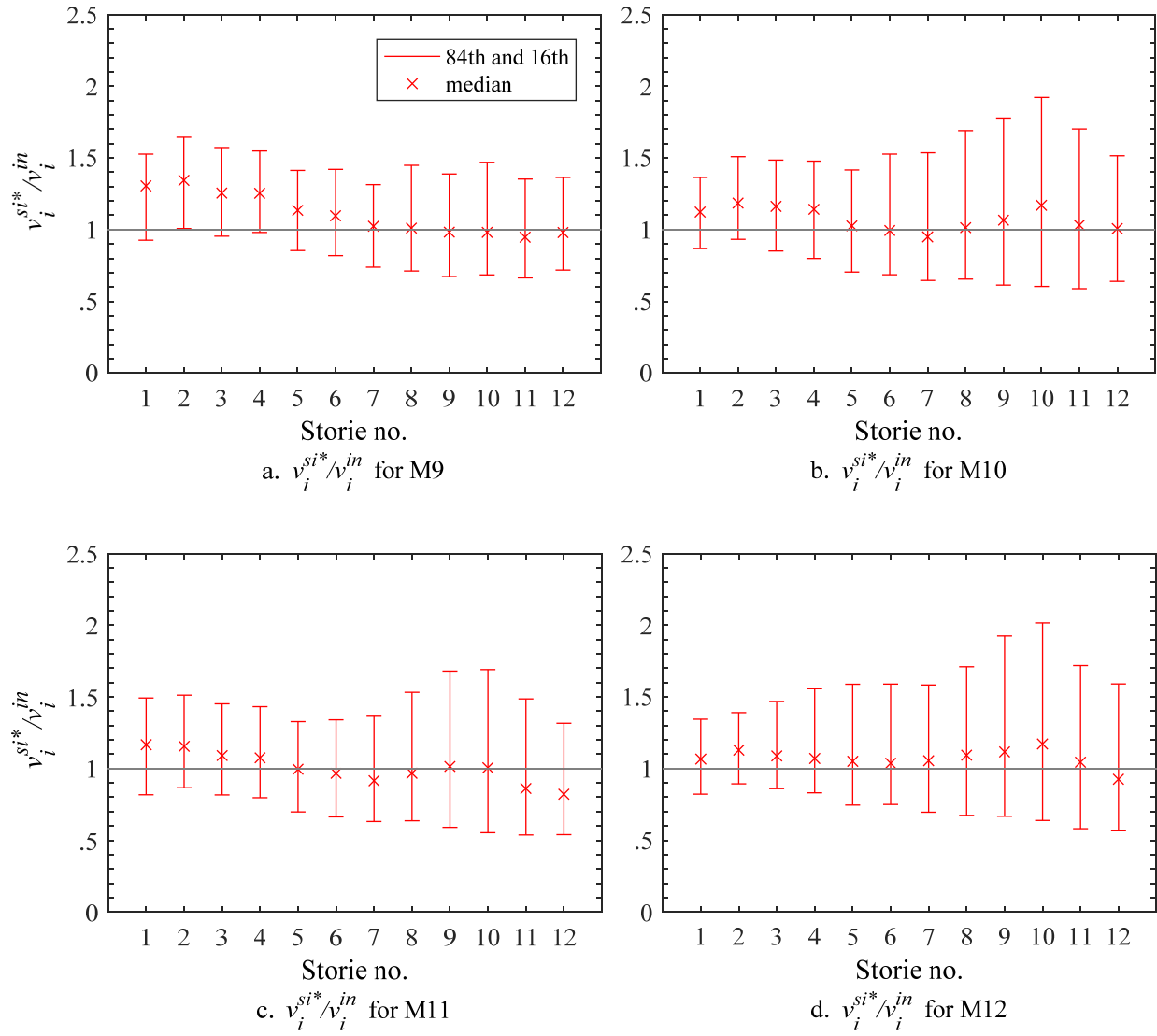


Figure 22. 84th, 50th, and 16th percentiles of v_i^{si*}/v_i^{ni} for twelve-story models.

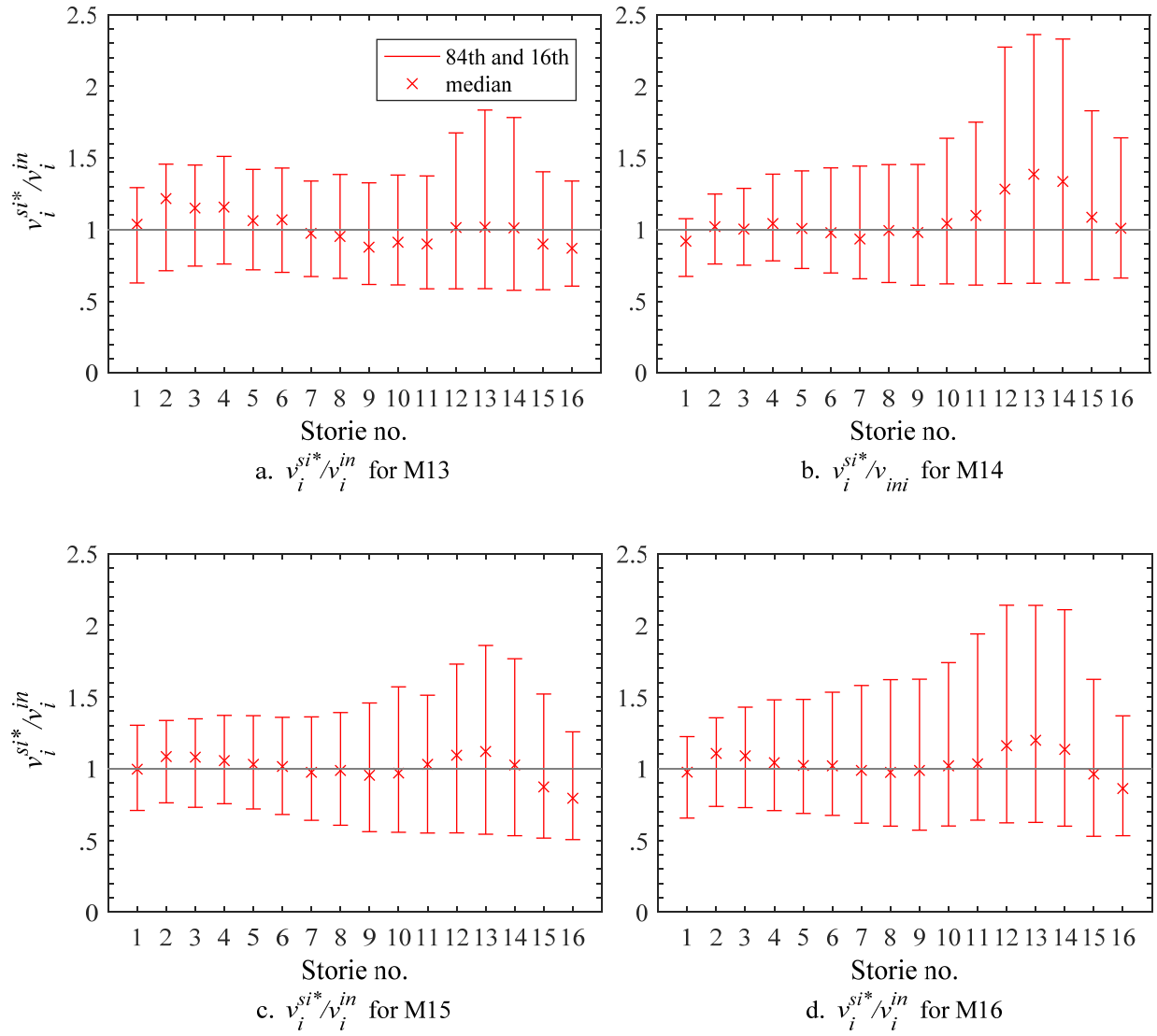


Figure 23. 84th, 50th, and 16th percentiles of v_i^{si*}/v_i^{ni} for sixteen-story models.

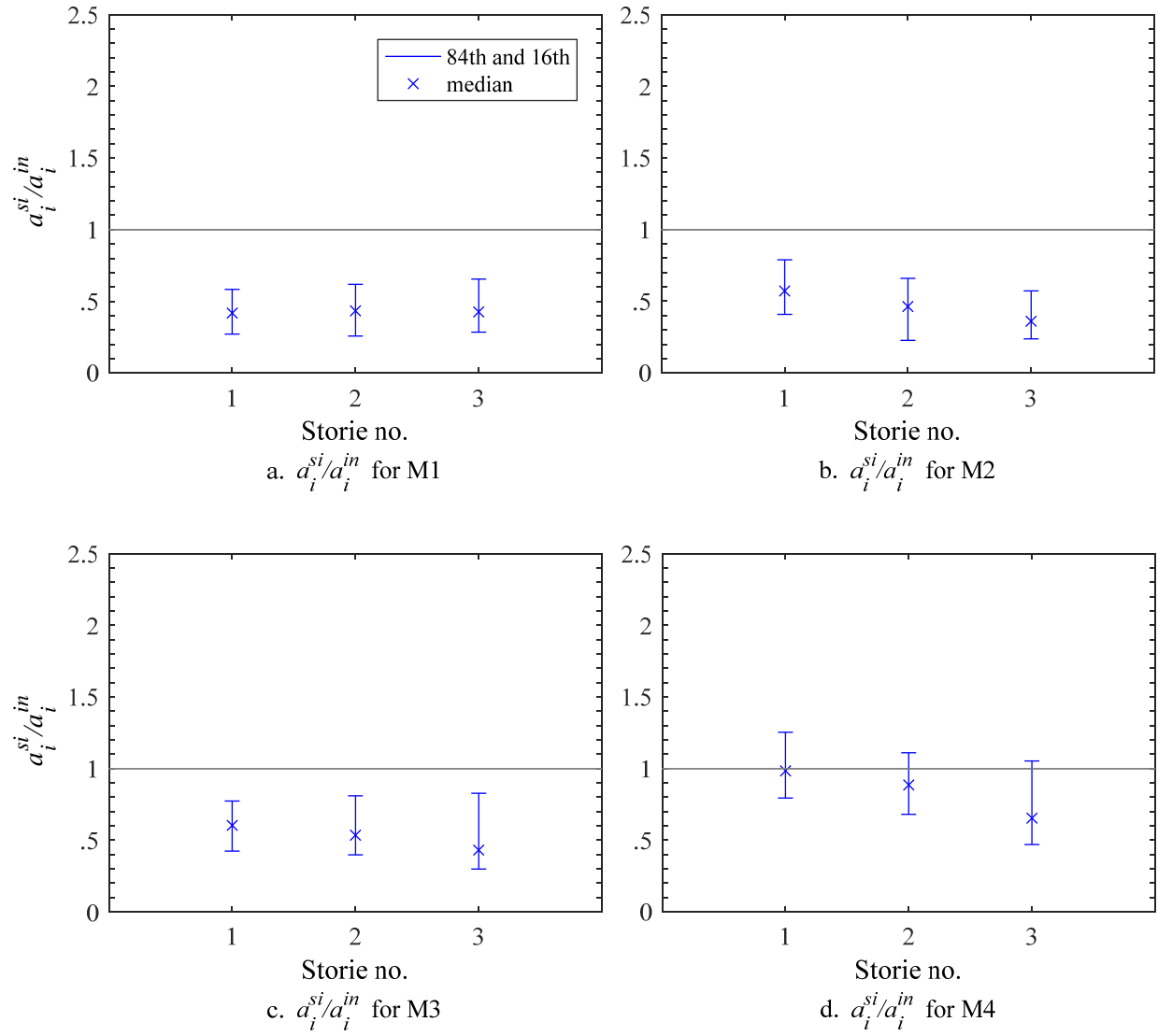


Figure 24. 84th, 50th, and 16th percentiles of a_i^{si}/a_i^{ni} for three-story models.

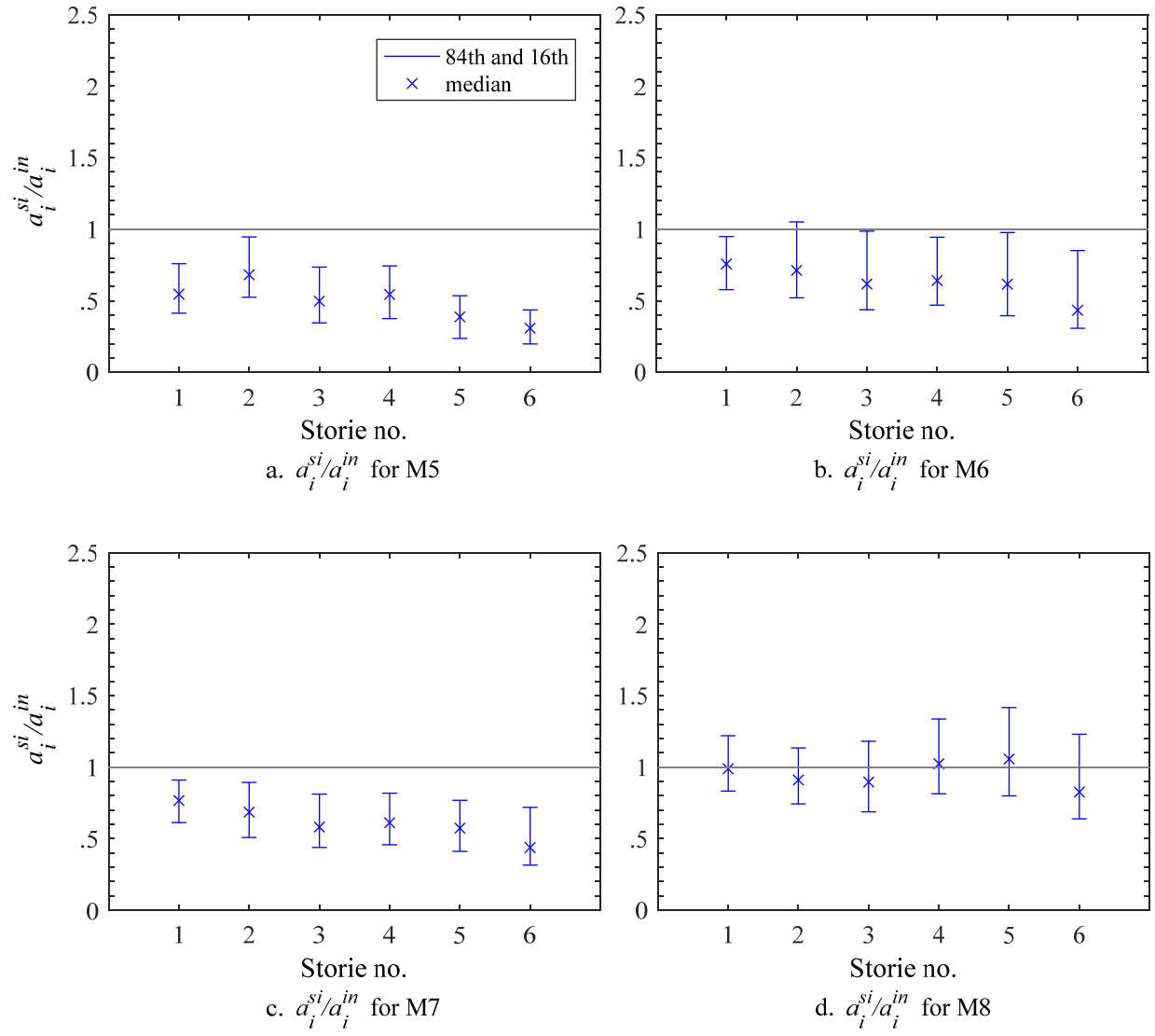
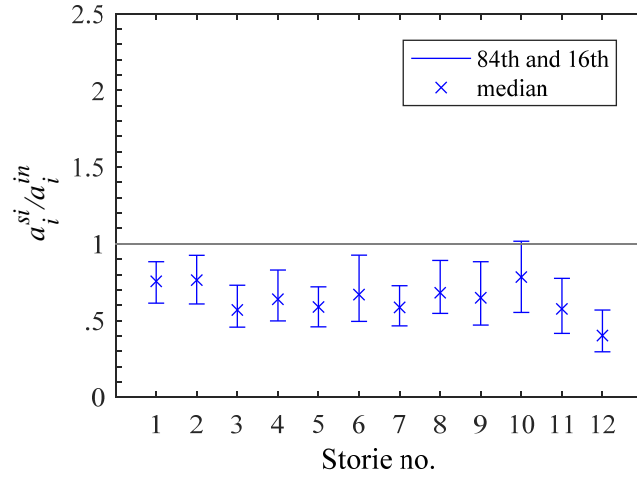
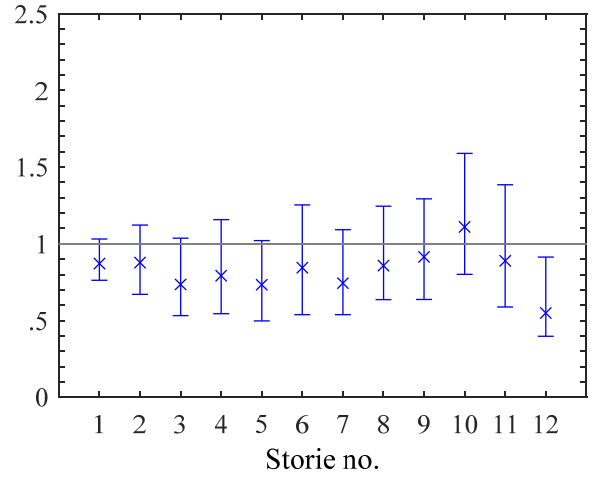


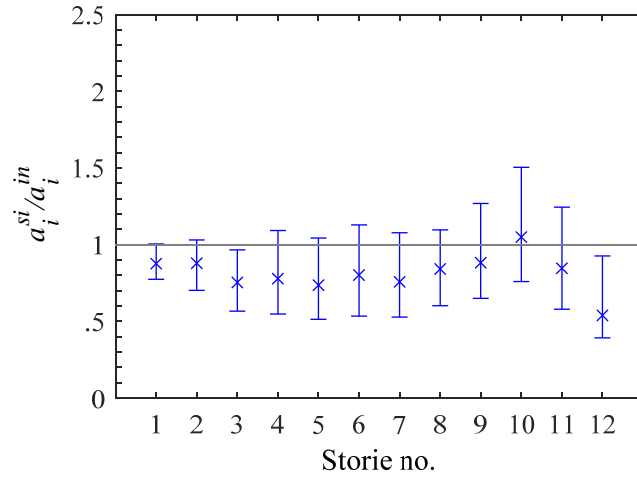
Figure 25. 84th, 50th, and 16th percentiles of a_i^{si}/a_i^{ni} for six-story models.



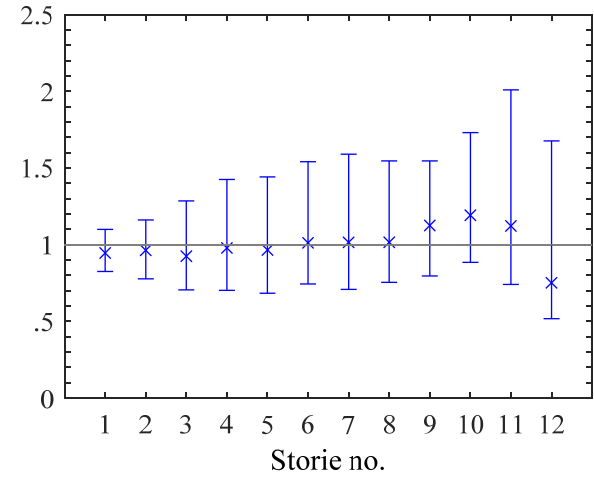
a. a_i^{si}/a_i^{in} for M9



b. a_i^{si}/a_i^{in} for M10

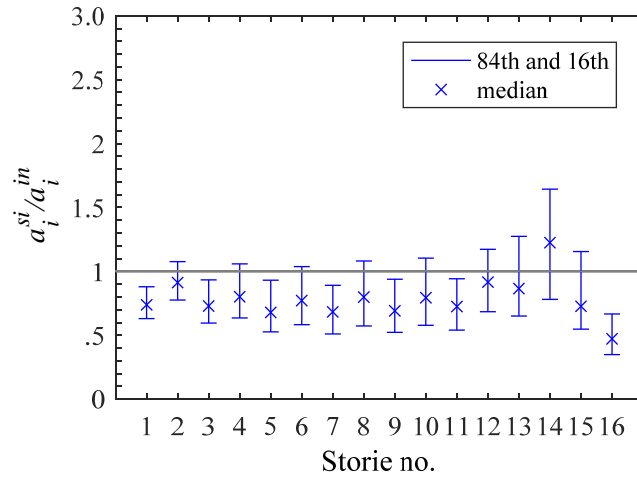


c. a_i^{si}/a_i^{in} for M11

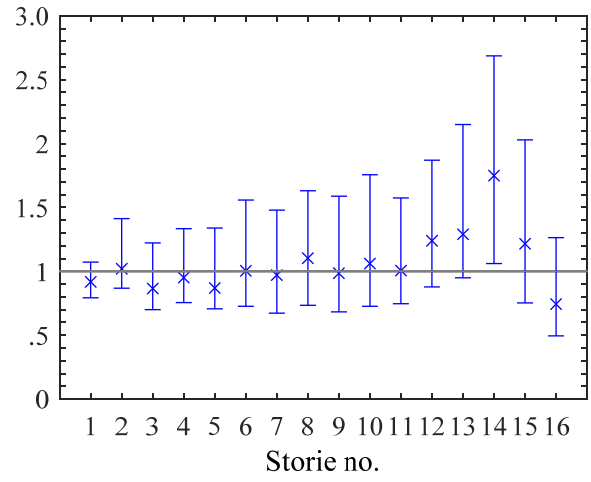


d. a_i^{si}/a_i^{in} for M12

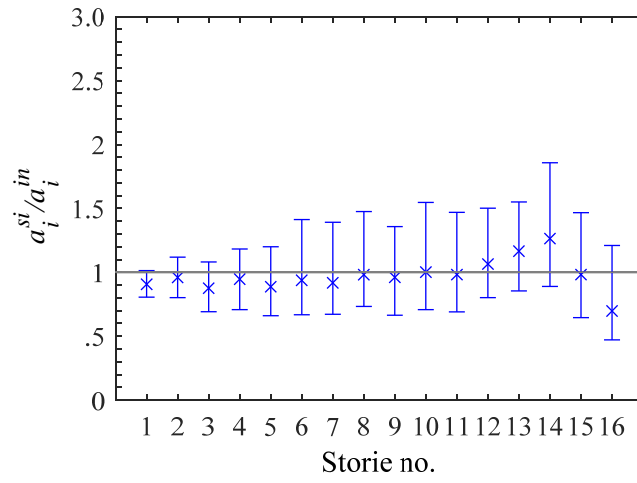
Figure 26. 84th, 50th, and 16th percentiles of a_i^{si}/a_i^{ni} for twelve-story models.



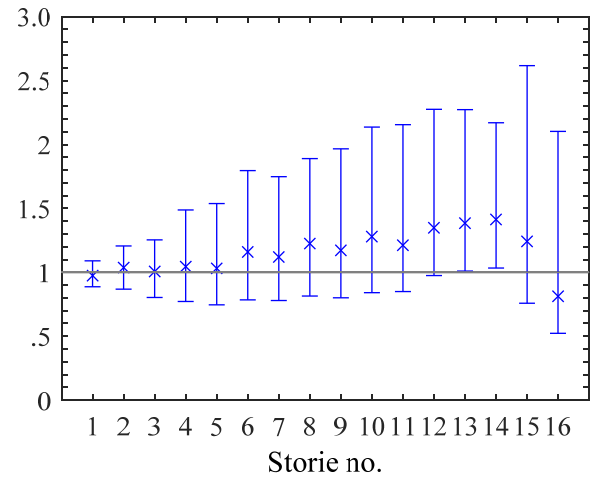
a. a_i^{si}/a_i^{in} for M13



b. a_i^{si}/a_i^{in} for M14



c. a_i^{si}/a_i^{in} for M15



d. a_i^{si}/a_i^{in} for M16

Figure 27. 84th, 50th, and 16th percentiles of a_i^{si}/a_i^{ni} for sixteen-story models.

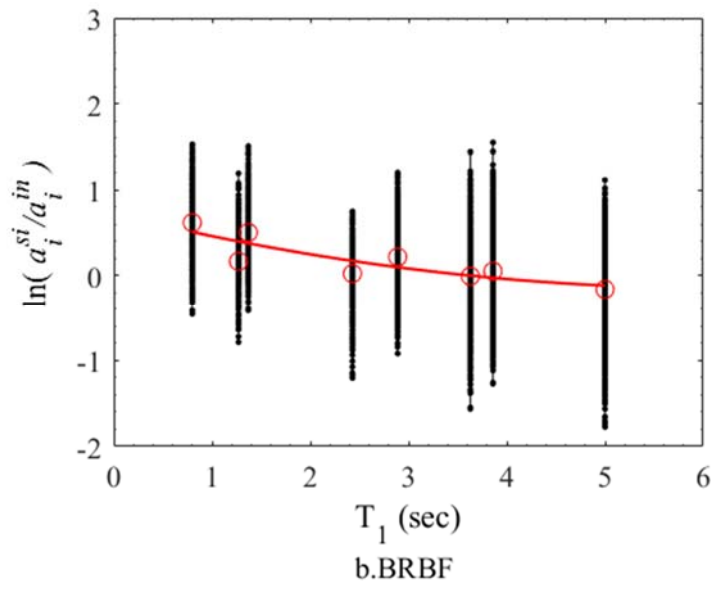
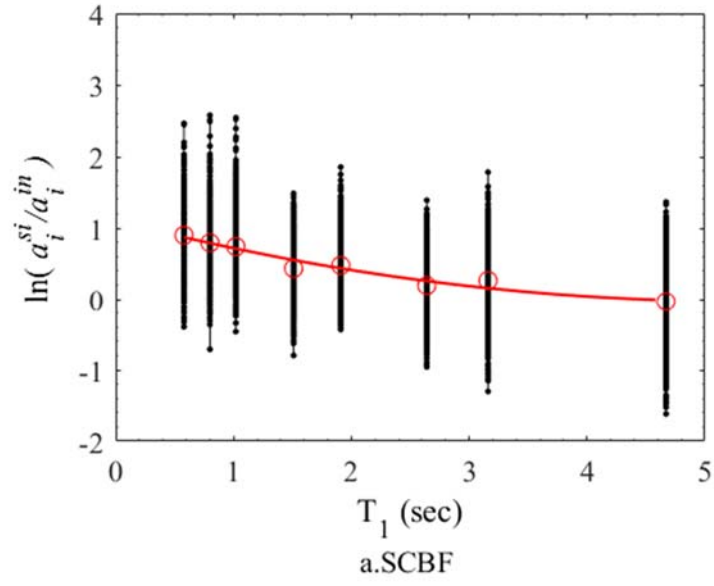
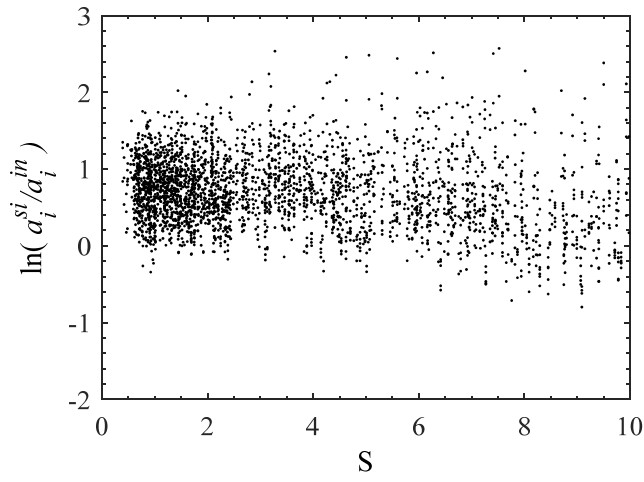
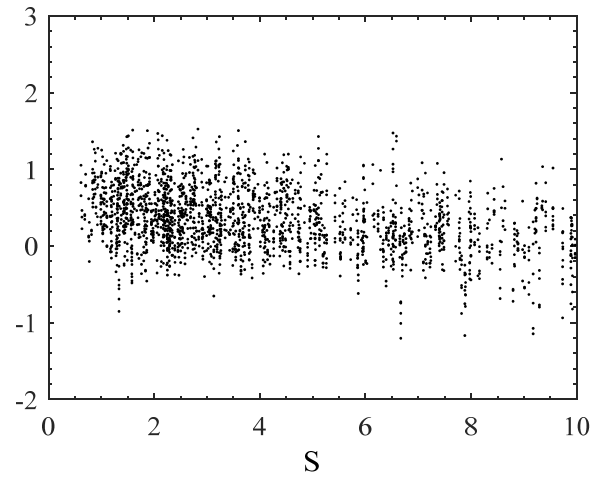


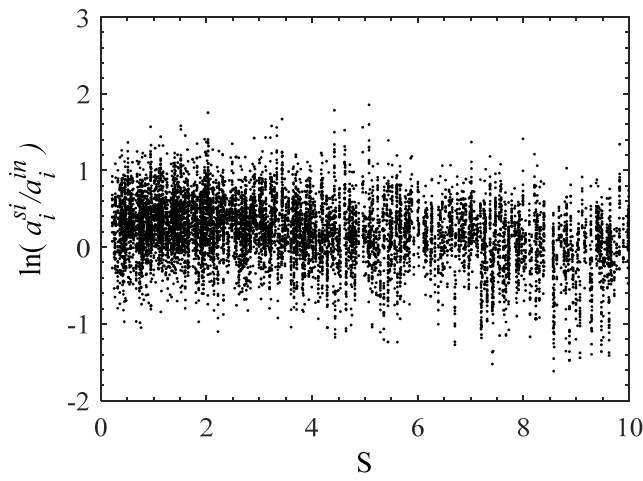
Figure 28. Inter-model residuals for a_i^{si}/a_i^{ni} as a function of T_1 and framing type.



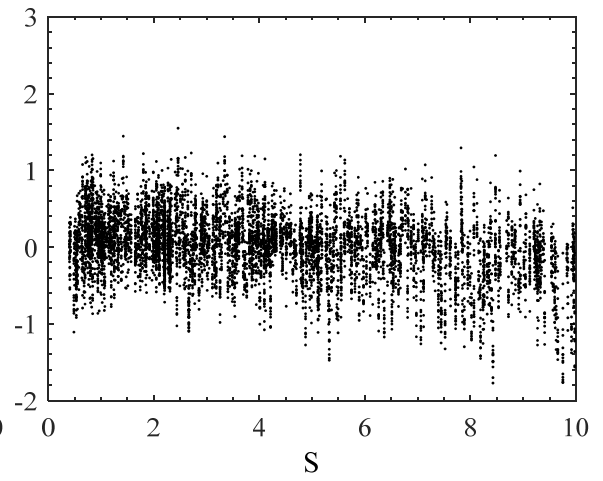
a.SCBF (M1,M2,M5,M6)



b.BRBF (M3,M4,M7,M8)



c.SCBF (M9,M10,M13,M14)



d.BRBF (M11,M12,M15,M16)

Figure 29. a_i^{si}/a_i^{ni} as a function of S and framing type.

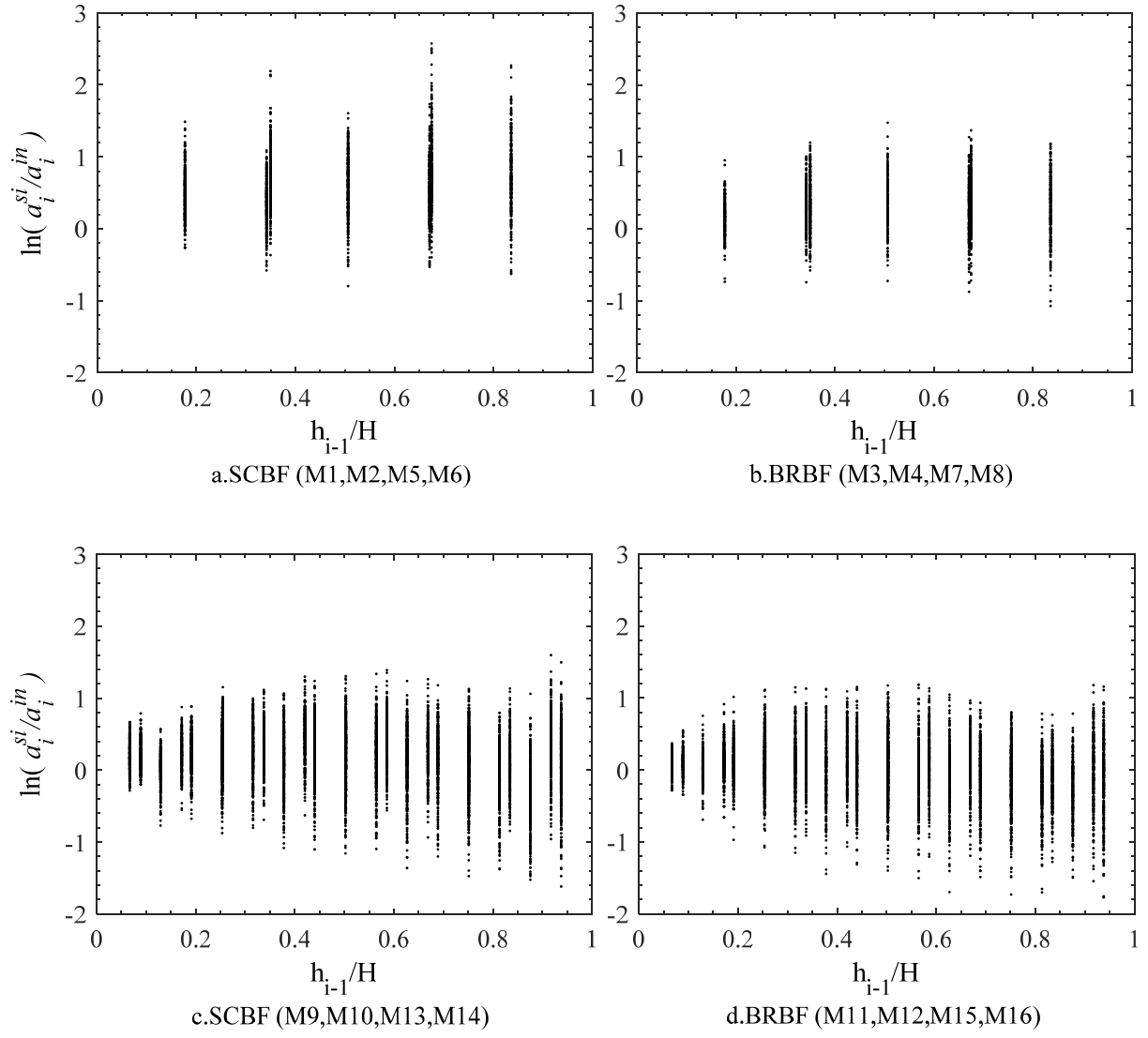


Figure 30. a_i^{sl}/a_i^{ni} as a function of h_i/H and framing type.

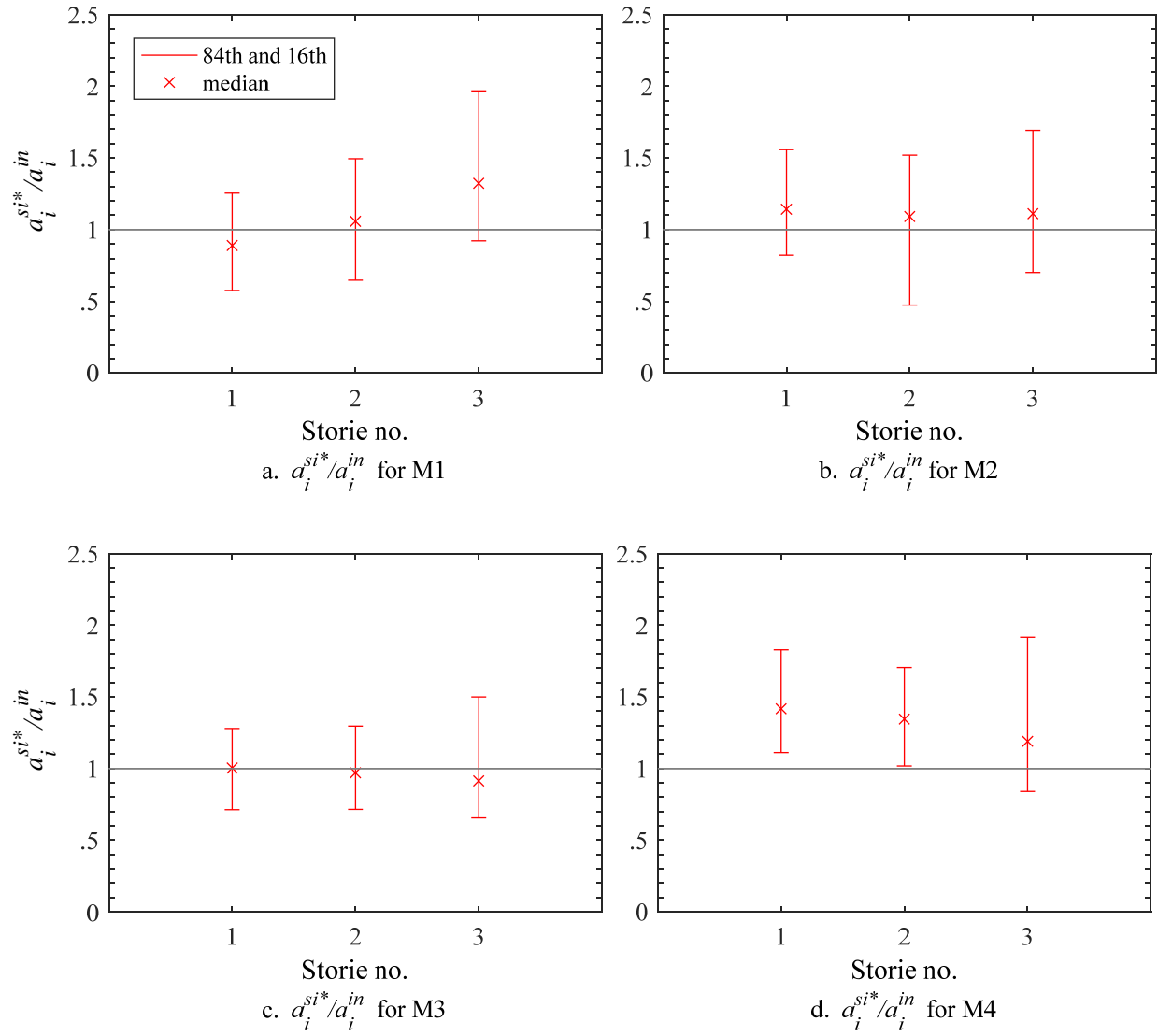


Figure 31. 84th, 50th, and 16th percentiles of a_i^{si*}/a_i^{ni} for three-story models.

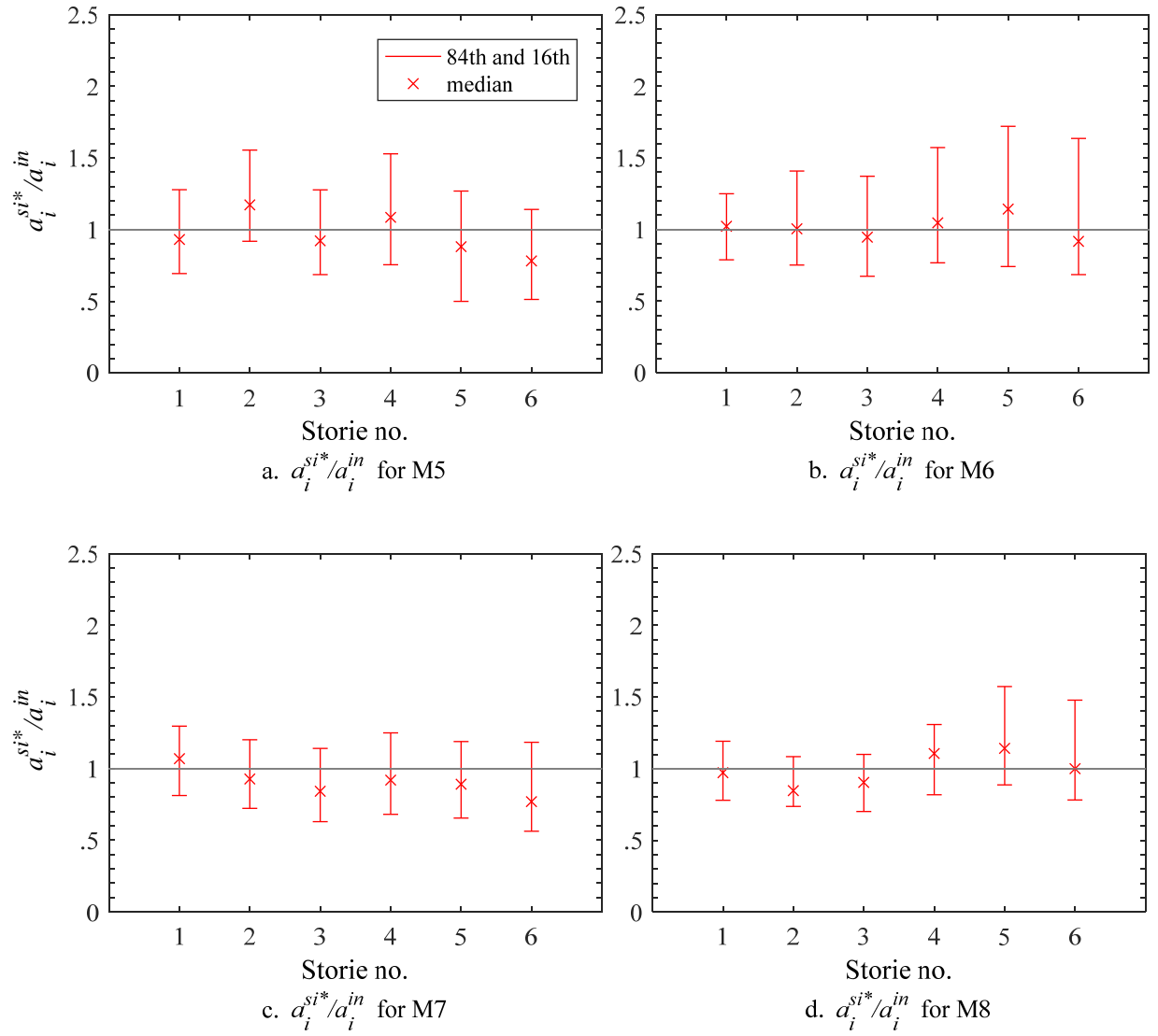


Figure 32. 84th, 50th, and 16th percentiles of a_i^{si*}/a_i^{ni} for six-story models.

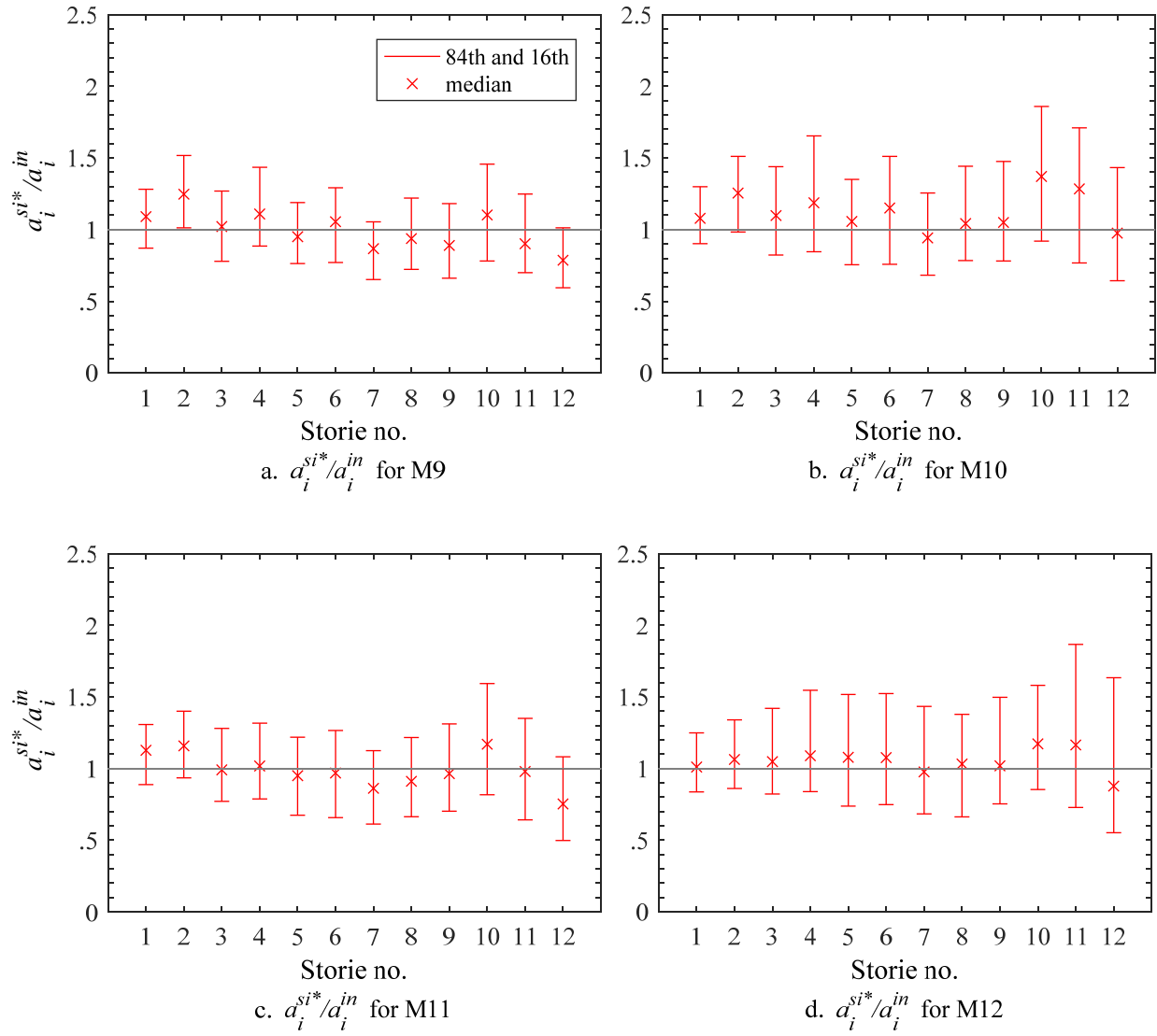
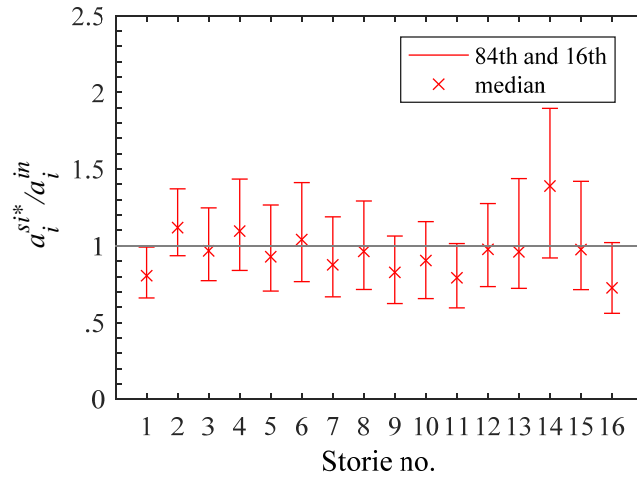
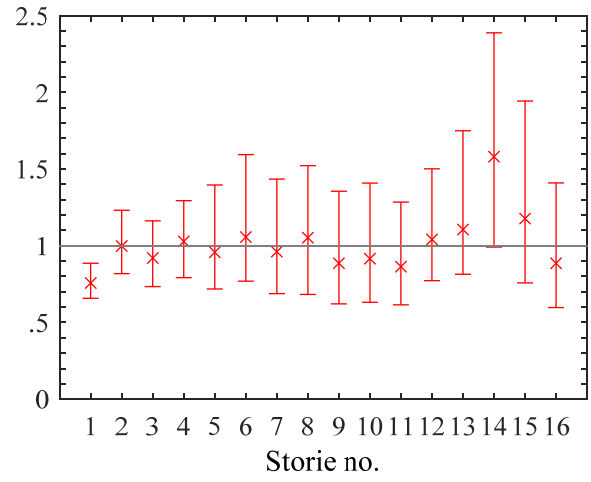


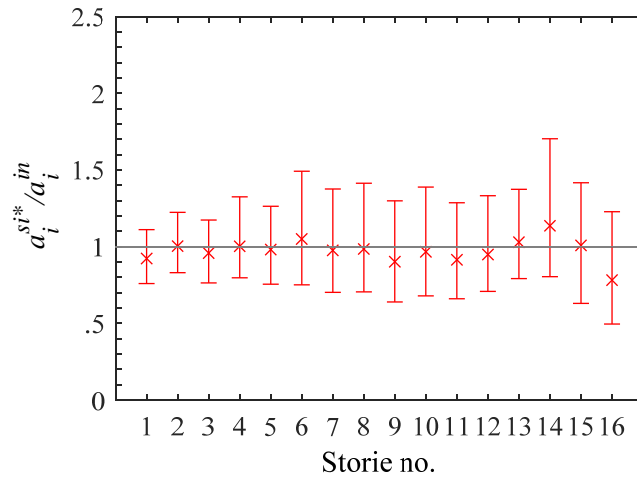
Figure 33. 84th, 50th, and 16th percentiles of a_i^{si*}/a_i^{ni} for twelve-story models.



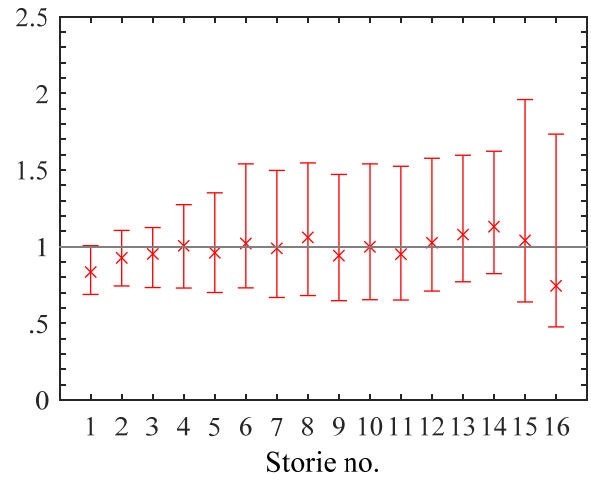
a. a_i^{si*}/a_i^{in} for M13



b. a_i^{si*}/a_{ini} for M14



c. a_i^{si*}/a_i^{in} for M15



d. a_i^{si*}/a_i^{in} for M16

Figure 34. 84th, 50th, and 16th percentiles of a_i^{si*}/a_i^{ni} for sixteen-story models.